中国科学技术大学
University of Science and Technology of China

Interferometry and Polarimetry in Magnetic Fusion Devices

WEIXING DING
University of Science and technology of China

Nagoya, Dec.11, 2024

Introduction to myself

- Chair professor at the University of Science and Technology of China (USTC), Hefei, China.
- PhD in 1991 at University of Science and Technology of China
- Alexander von Humboldt Fellow (1994-1996)
- Research fellow at University of Saskatchewan in Canada (1996-1997)
- Post-doctor fellow at Oak Ridge National Laboratory, Oak Ridge, TN,USA (1997-1999)
- Researcher at University of California, Los Angeles, CA, USA (2000-2018)

- Fellow of the American Physical Society (APS fellow 2010)
- Research interests : magnetic confinement plasma physics and the development of plasma diagnostics (e.g. interferometer and polarimeter).

Acknowledgement

M.A. Van Zeeland[1], T.N. Carlstrom[1], D. Du[1], A. Gattuso[1], F. Glass[1], P. Mauzey[1], C. Muscatello[1], R.C. O'Neill[1], M. Smiley[1], J. Vasquez[1], D.L. Brower[2], J. Chen[2] ,Y.Q.Chu[2] , W. F. Bergerson[2] ,D. Finkenthal[3], A. Colio[3] , [4]D. Johnson, [4]R. Wood, [5]C. Watts, P. Xu[6], J. H. Irby[6] , T.Lan[7],H.Zhang[7] , Z.Q. Bai[7], Z.L. Mao[7] ,W.Mao[7],Q.F.Zhang[7] , J.L.Xie[7] ,G.Zhuang[7] , H. Q. Liu[8], Y. X. Jie[8], Z. Y. Zou[8], J. P. Qian[8], W.M. Li[8], Y. Yang[8], X. C. Wei[8], T. Lan[8], H.Lian[8]

[1]*General Atomics , San Diego, USA*
[2]*University of California, Los Angeles, USA*
[3]*Palomar Scientific Instruments , USA*
[4]*PPPL*
[5]*ITER Organization*
[6]*Massachusetts Institute of Technology, Cambridge, MA, USA*
[7]*University of Science and Technolodge of China*
[8]*Institute of Plasma Physics, Chinese Academy of Sciences*

Part I: Interferometer

(1) Basics and wave length selection for magnetized plasmas;

(2) Homodyne Optical Fiber Interferometer for a θ-pinch (λ =1.55 μm);

(3) Tangential Interferometry and Polarimetry (TIP) for ITER (λ =10.6 μm);

(4) Dispersion Interferometer for EAST (λ =9.27 μm);

(5) Solid-State source-based interferometer on KTX-RFP (λ =461 μm).

Part II Polarimeter

- **Two wave polarimetry (Faraday effect and Cotton-Mouton effect) on C-mode (λ=117μ m);**

- **Three wave interferometer and polarimetry on EAST (λ =432 μm);**

- **Tangential Interferometer and Polarimetry (TIP) for ITER (λ =10.6 μm);**

- **PoPola Polarimetry for ITER (λ =119 μm);**

- **The application of line-integrated measurement to plasma vertical position.**

Part III Notes

(a) Dispersion relation for hot plasmas;

(a) Coupling between Cotton-Mouton and Faraday rotation;

(b) Coupling between Interferometer and Polarimetry .

Interference of Electromagnetic Waves

Interference is the phenomenon there are constructive or destructive patterns due to multiple waves meeting and superimposing in space.

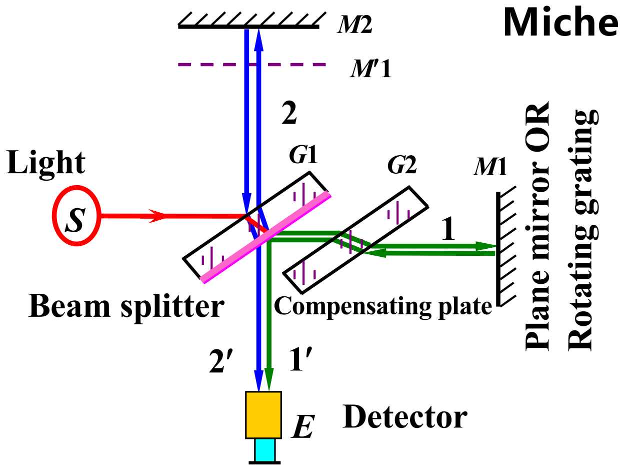

Michelson interferometer

- **There are two monochromatic waves:**

$$E_1 = E_{10}\cos(\omega t + \emptyset_1)$$

$$E_2 = E_{20}\cos(\omega t + \emptyset_2)$$

- **The two waves superimposing:**

$$I \sim |E_1 + E_2|^2 = E_{10}^2 + E_{20}^2 + 2E_{10}E_{20}\cos(\Delta\emptyset) = A + B\cos(\Delta\emptyset)$$

$$\Delta\emptyset = \emptyset_2 - \emptyset_1 = \frac{\omega}{c} N\Delta l \quad (\text{refractive index } N = \frac{c}{v_p})$$

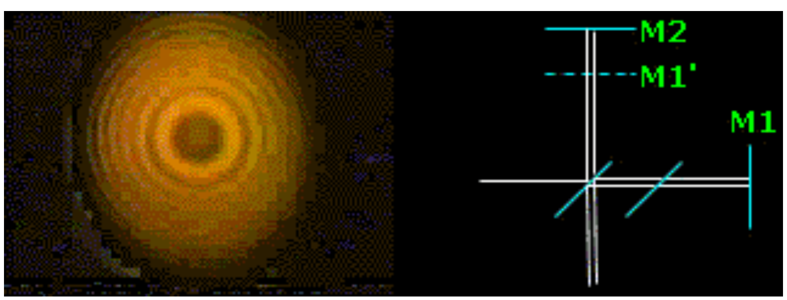

The intensity I varies with the phase difference $\Delta\emptyset$ (or ΔL) .

Two Common Interferometer Techniques

❑ Michelson interferometer

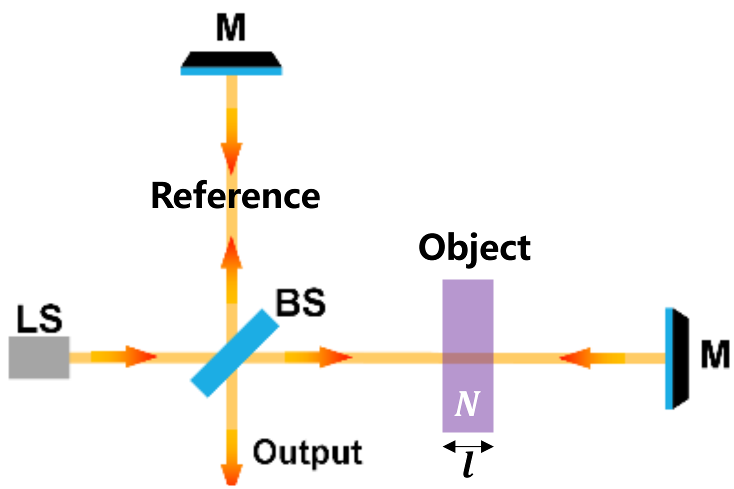

$$\Delta\emptyset = \frac{\omega}{c}(N-1)\Delta 2l$$

❑ Mach-Zehnder interferometer

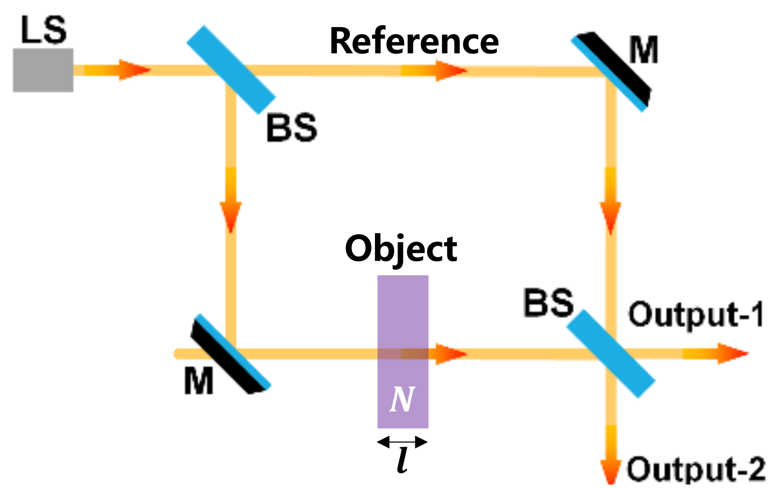

$$\Delta\emptyset = \frac{\omega}{c}(N-1)\Delta l$$

➢ When the laser frequency ω and the object thickness l are known, the refractive index N can be obtained by measure the phase difference $\Delta\emptyset$.

Electromagnetic Waves in Vacuum and Plasmas

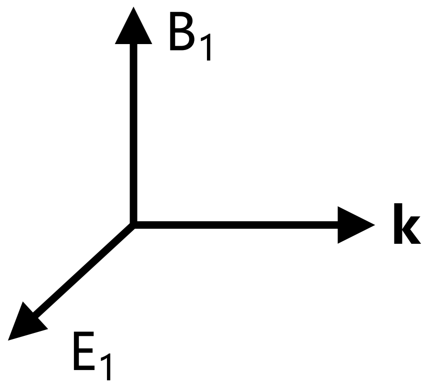

$$\nabla\times E_1 = -\frac{\partial B_1}{\partial t}$$ Farady law

$$c^2\nabla\times B_1 = \frac{\partial E_1}{\partial t} + j_1/\varepsilon_0$$ Ampere’s law

$$j_1 = -en_e v_{e1}$$

$$m_e\frac{\partial v_{e1}}{\partial t} = -eE_1$$

Speed of light ($\frac{c}{N}$ or refaractivity) changes with electron density in plasmas.

Measurement of light speed in plasmas is a fundamental principle for interferometer and polarimetry application

Dispersion Relations for Electromagnetic Waves in Magnetized Plasmas

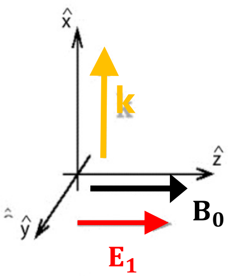

- $\boldsymbol{k} \perp \boldsymbol{B_0}$ **(For high-frequency EM waves: $\boldsymbol{\omega \gg \omega_{pe}, \omega_{ce}}$)**

$\boldsymbol{E_1} \parallel \boldsymbol{B_0}$**: Ordinary wave (O-mode)**

$$N_O^2 = 1 - \frac{\omega_{pe}^2}{\omega^2} \xrightarrow{\text{Taylor expansion}} N_O = 1 - \frac{1}{2}\frac{\omega_{pe}^2}{\omega^2}$$

Interferometer

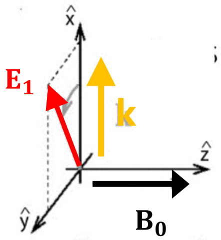

$\boldsymbol{E_1} \perp \boldsymbol{B_0}$**: Extraordinary wave (X-mode)**

$$N_X^2 = 1 - \frac{\omega_{pe}^2}{\omega^2}\frac{\omega^2 - \omega_{pe}^2}{\omega^2 - \omega_{pe}^2 - \omega_{ce}^2} \xrightarrow{\text{Taylor expansion}} N_X = 1 - \frac{1}{2}\frac{\omega_{pe}^2}{\omega^2} - \frac{1}{2}\frac{\omega_{pe}^2}{\omega^2}\frac{\omega_{ce}^2}{\omega^2}$$

Cotton-Mouton effect Polarimetry

- $\boldsymbol{k} \parallel \boldsymbol{B_0}$

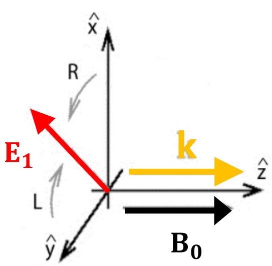

Right-handed wave (R-wave) and left-handed wave (L-wave):

$$N_{R,L}^2 = 1 - \frac{\omega_{pe}^2}{\omega^2(1 \pm \frac{\omega_{ce}}{\omega})} \xrightarrow{\text{Taylor expansion}} \begin{cases} N_R = 1 - \frac{1}{2}\frac{\omega_{pe}^2}{\omega^2}(1 + \frac{\omega_{ce}}{\omega}) \\ N_L = 1 - \frac{1}{2}\frac{\omega_{pe}^2}{\omega^2}(1 - \frac{\omega_{ce}}{\omega}) \end{cases}$$

Faraday-effect Polarimetry

Interferometer –Plasma Density Measurement

Phase shift relates to plasma density n_e

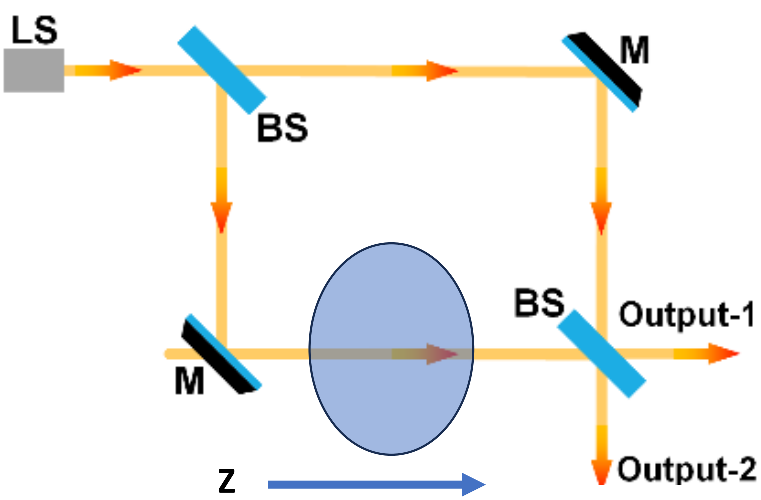

Ref. Chord

Signal chord

- **Probing beam (plasma):** $(\omega \gg \omega_{pe})$

$$N = 1 - \frac{1}{2}\frac{\omega_{pe}^2}{\omega^2} \qquad \omega_{pe}^2 = \frac{n_e e^2}{m_e \varepsilon_0}$$

- **Reference beam (vacuum, air):**

$$N_0 \sim 1 \quad (constant)$$

- **Phase difference between reference beam and probing beam**

$$\Delta\varphi = \frac{2\pi}{\lambda}\int_{Z_1}^{Z_2}[N(z) - N_0(z)]dz$$

$$\Delta\varphi = 2.82\times10^{-15}\lambda\int n_e dl$$

$$+\frac{2\pi}{\lambda}N_0\Delta l$$

If optical paths are changed due to vibration or thermal expansion

Phase difference $\Delta\varphi$ is proportional to the path integral of the electron density n_e.

Wave Length Selection for Interferometer

Some wavelength selection constrains

a) **Frequency $(\omega \gg \omega_{pe})$, but shorter wavelength is subject to vibrations and has less phase change;**

The Cut-off density:

$$n_c = \frac{\omega^2 m_e \varepsilon_0}{e^2}$$

b) **Long wavelength has more phase change, but probing beam may be deflected due to density gradient; For a cylindrical plasma the angle of refraction**

$$\alpha(x) \simeq \frac{n_0}{n_c}\frac{2x}{a^2}\sqrt{a^2 - x^2} \approx \left[\frac{e^2}{(4\pi^2 c^2 \varepsilon_e m_0)}\right] n_0 \lambda^2$$

c) **One also has to consider availability of light sources and detectors.**

Density Profile on EAST Tokamak $10^{19}/m^3$

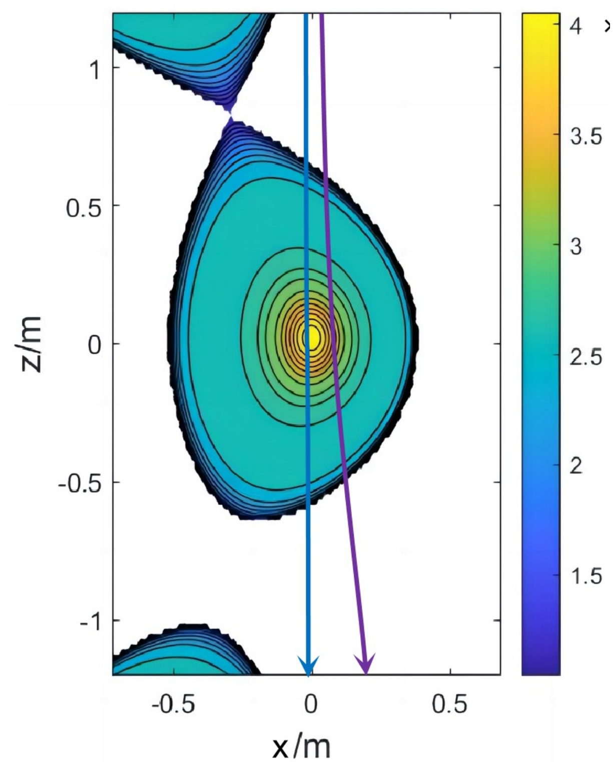

50xα

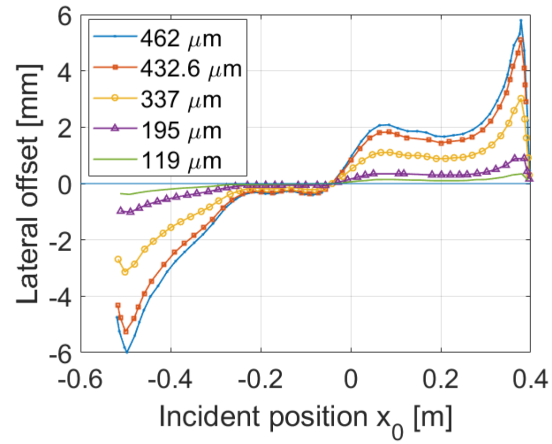

Beam offset

The higher density is , the shorter wavelength you select

Compromise among phase resolution, vibration, refraction and light sources

Interferometer –Density Measurement

Homodyne and Heterodyne Techniques

Homodyne Optical Fiber Interferometer (1.55μm)

3×3 optical coupler can be treated as a $\frac{2\pi}{3}$ phase demodulator

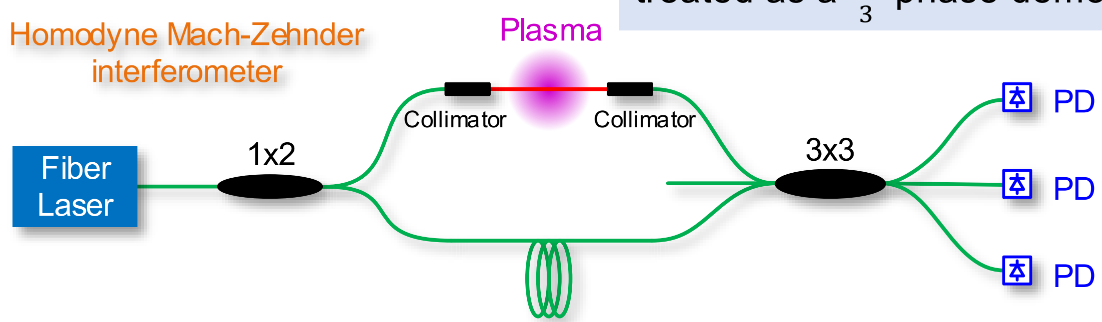

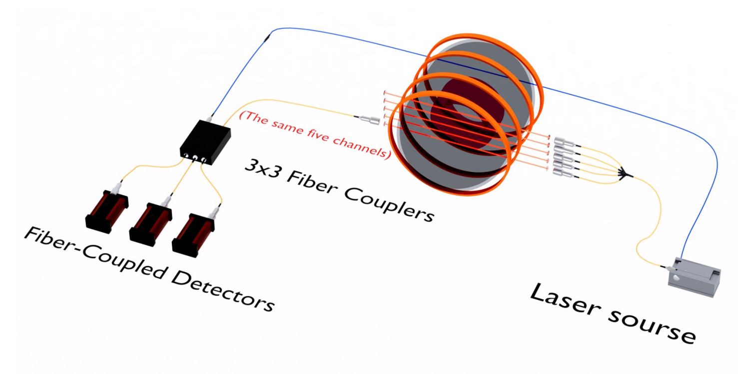

$$\begin{cases} I_1 = I_A + I_B cos(\varphi) \\ I_2 = I_A + I_B cos\left(\varphi + \frac{2\pi}{3}\right) \\ I_3 = I_A + I_B cos\left(\varphi - \frac{2\pi}{3}\right) \end{cases}$$

$$\varphi = \tan^{-1}\left(\frac{\sqrt{3}(I_2 - I_3)}{2I_1 - I_2 - I_3}\right)$$

$$\varphi = -\lambda\, r_e \int n_e\, dL$$

Simple setup provides density measurement for theta-pinch

Homodyne Optical Fiber Interferometer For θ-pinch

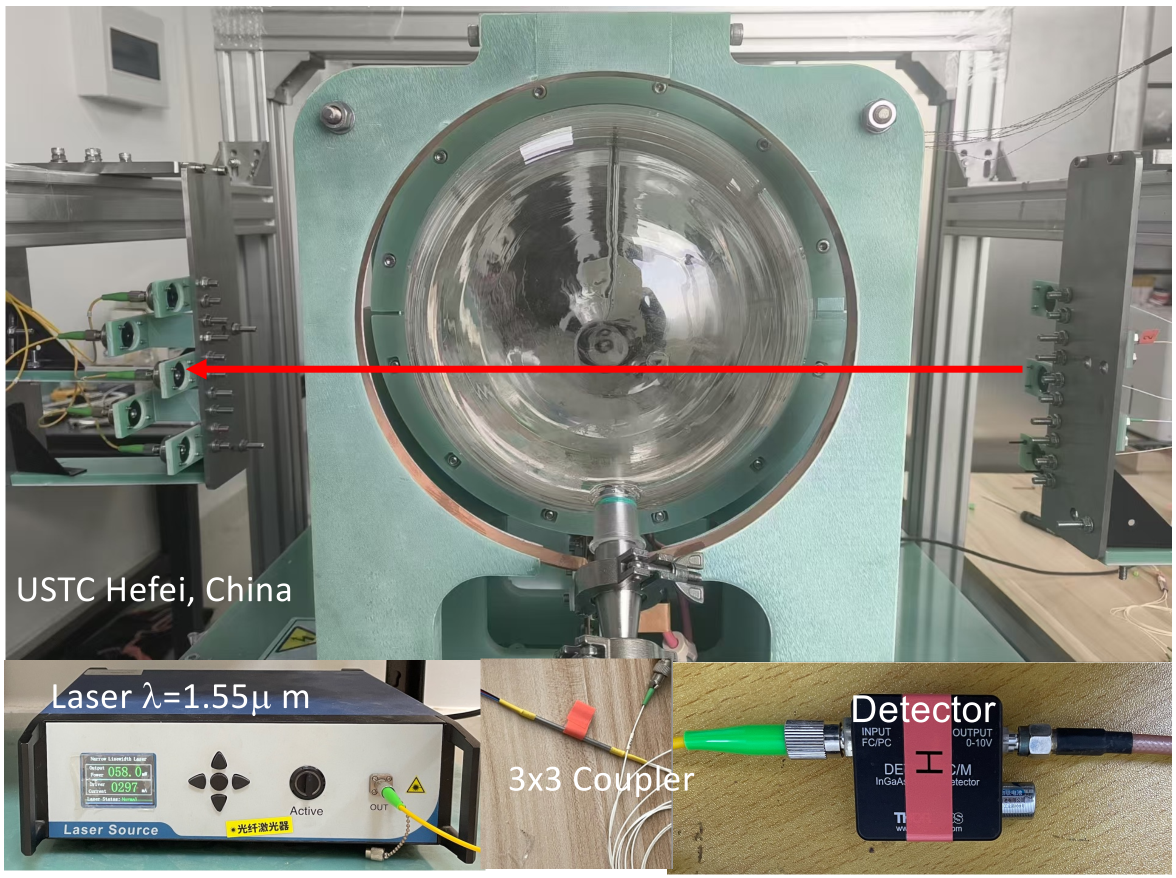

T. Lan, Z. Bai, H. Zhang, et al., Rev. Sci. Instrum. 95, 103514 (2024).

Density measurement of θ-pinch plasmas

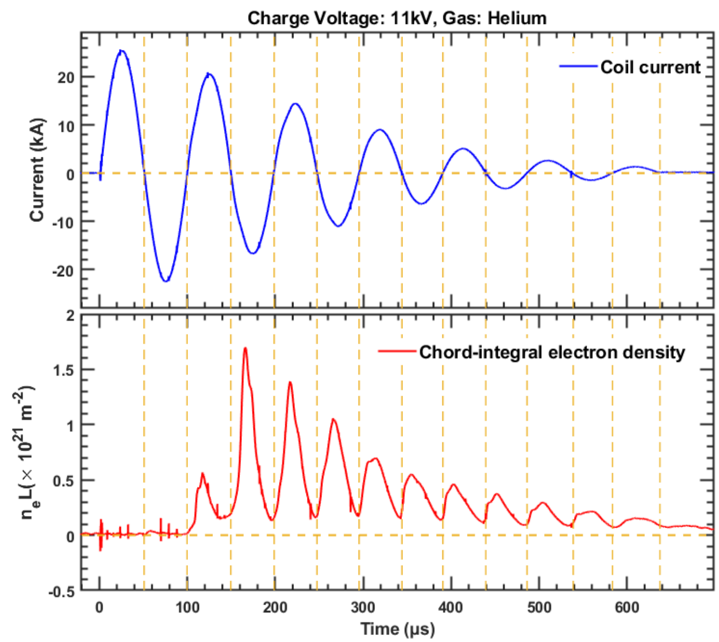

Here vibration and pathlength changes are negligible due to short time scale !

Optical Fiber Interferometer : Cons vs Pros

Pros:

- **Excellent sensitivity and a large dynamic range. Immunity to electromagnetic interference.**
- **Compact size with rugged packaging, and low cost .**

Cons:

- **Application from visible to near infrared wavelength, wavelength is suitable for high plasma density measurements (such as Pinch, Compact torus and magnetic inertial fusion etc) not tokamak plasmas;**
- **Vibration, low frequency noise (no frequency modulation) etc .**

$$\varphi = -\lambda\, r_e \int n_e\, dL$$

Such a simple setup doesn't work for long pulse tokamak plasmas!

Interferometer for Tokamak Plasmas

TIP is One of the Primary Density Diagnostics on ITER

Toroidal Interferometer/Polarimeter (TIP)

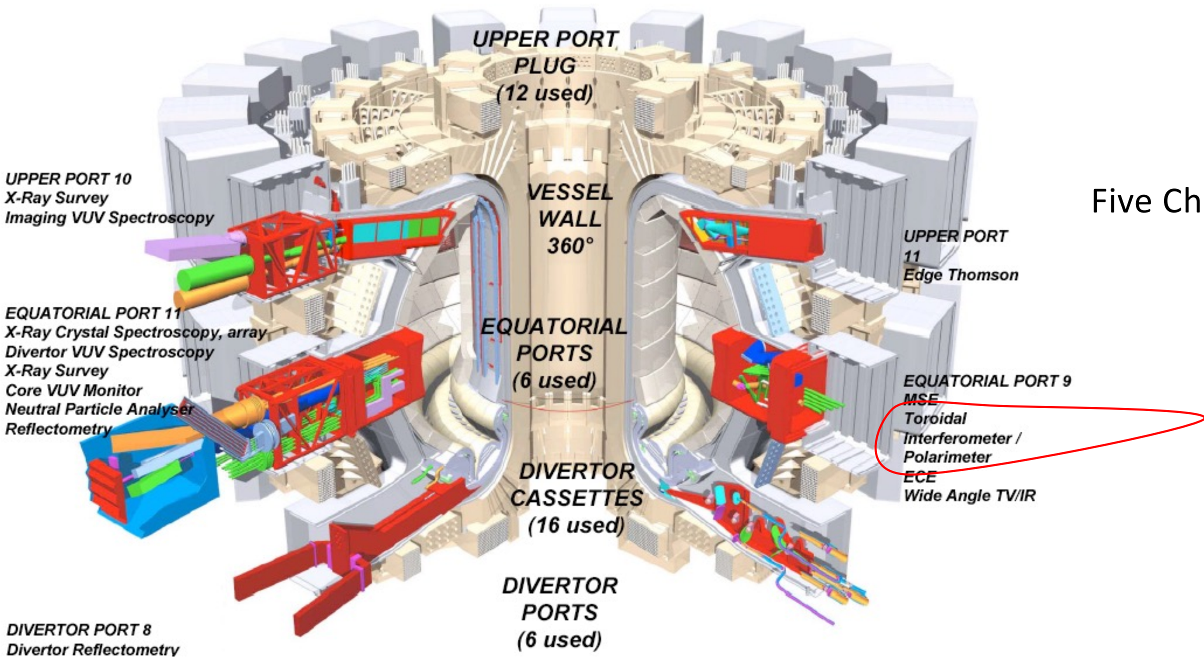

Partial Diagnostics (by the United States) on ITER

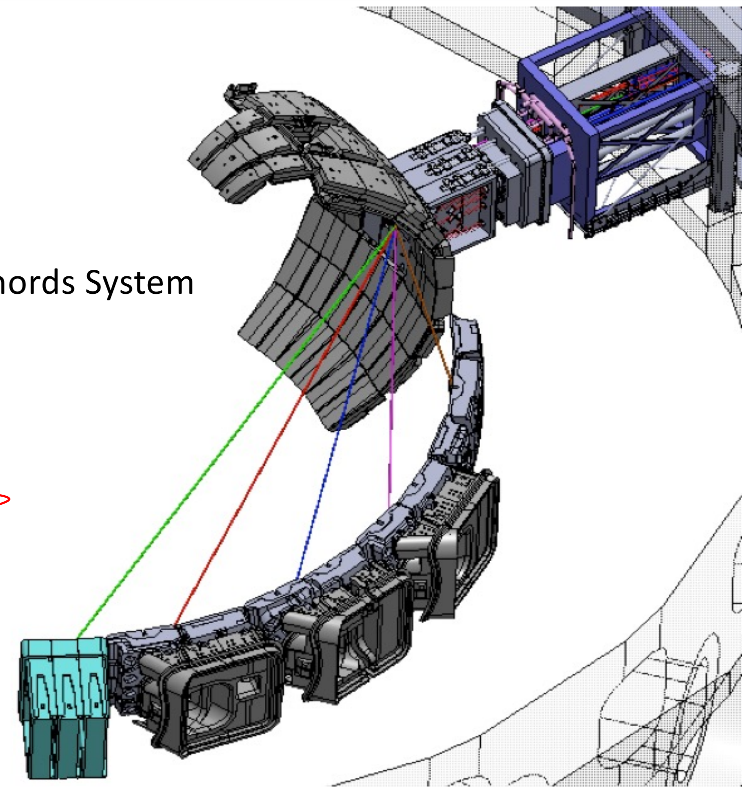

M. A.Van Zeeland, et al. RSI, 2013

CO_2 7W laser 10.6μm and 150mW 5.22 μm Quantum Cascade laser

Two-Color Interferometer For ITER TIP

- **Interferometer phase shift between the plasma and reference legs is caused primarily by mechanical vibrations and plasma index of refraction**

$$\varphi = -\lambda\, r_e \int n_e\, dL + \frac{2\pi}{\lambda} N_0 \Delta l$$

Vibration phase 10-100 x phase from plasma
Or path length change in a long pulse discharge

- **To separate the vibration and plasma phase shifts, two lasers at different wavelengths are used in each leg**

$$\int n_e dL = \frac{\lambda_{CO2}}{r_e(\lambda_{CO2}^2 - \lambda_{QCL}^2)}\left[\phi_{CO2} - \frac{\lambda_{QCL}}{\lambda_{CO2}}\phi_{QCL}\right]$$

10.59 μm CO2 laser   5.22 μm QCL laser

Vibration compensation is usually needed for short wavelength interferometer in long pulse plasmas like tokamaks

Basic Elements of TIP Interferometry Measurement – With Vibration Compensation Added

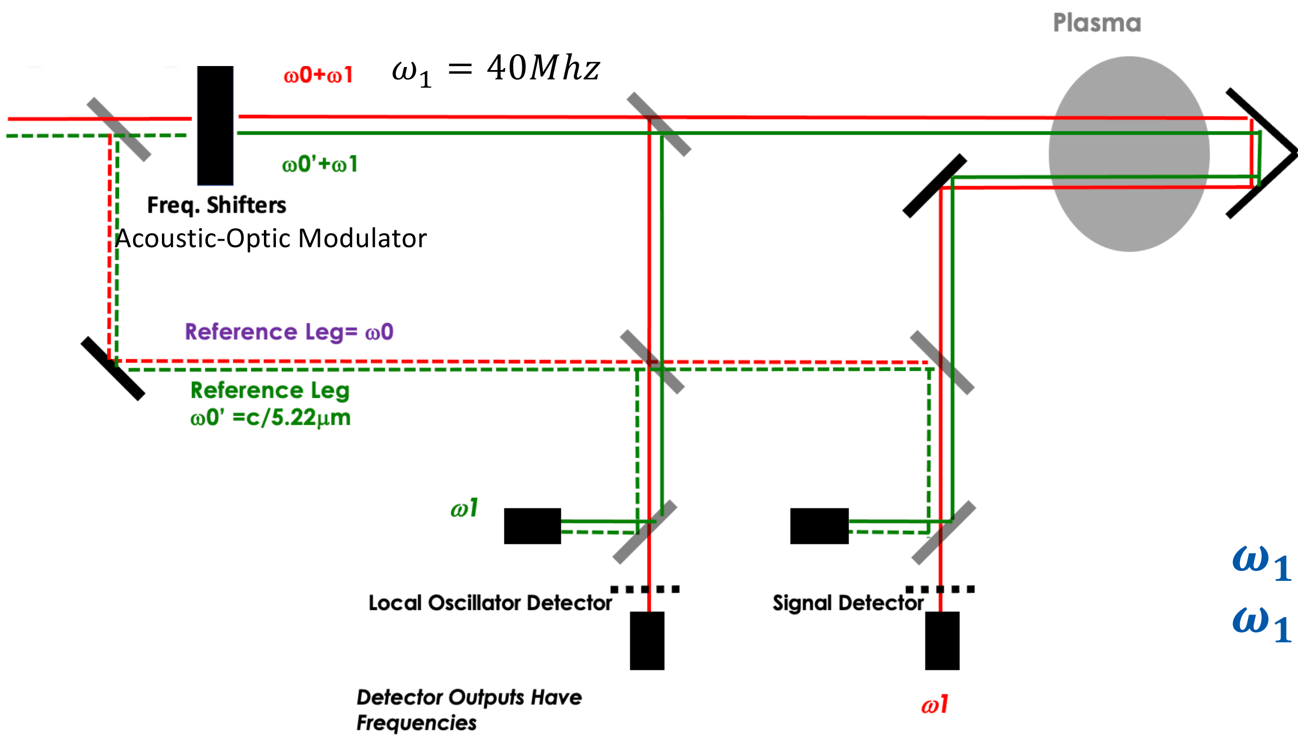

10.6 μ m (ω_0) and 5.22 μm (ω_0')

Two-Color

down shift frequency to low intermediate frequency (IF)

$$I_1 = I_A + I_B\cos(\omega_1 t + \varphi)$$

ω_1=0 Homodyne measurement

$\omega_1 \neq 0$ Heterodyne measurement

Basically two different wavelength interferometers are working together.

Two-Color Interferometer Measurements for DIII-D Plasmas

- **Total interferometer phase by vibration 10^4-10^5 Deg. much greater than phase shift by DIII-D plasmas.**

- **Plasma induced phase shifts in DIII-D < 800 Deg.**
- **Phase noise/ or uncertainty is low**
  - **$\delta\phi_{int} < 2°$ (ITER flattop ϕ_{int}~3000°)**

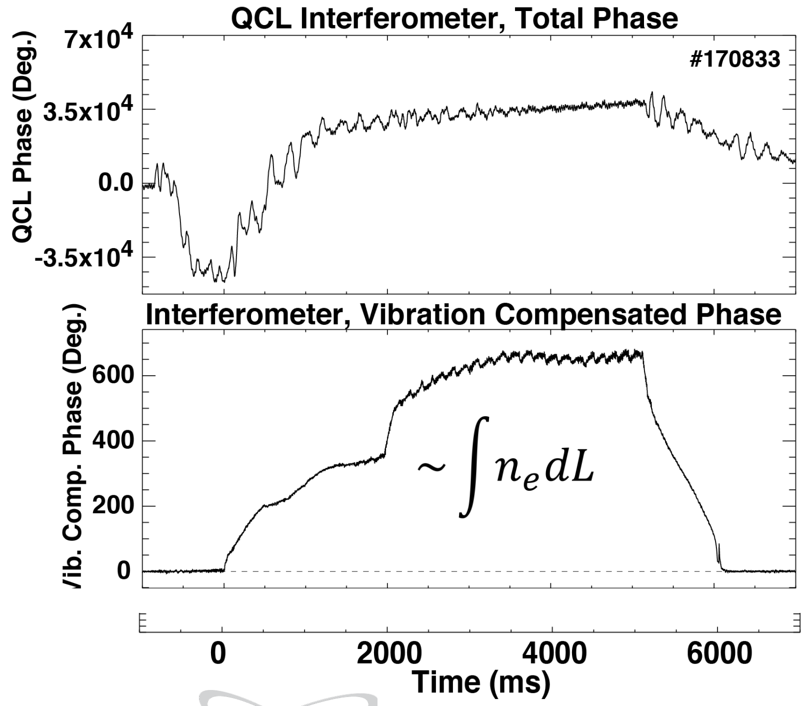

DIII-D NATIONAL FUSION FACILITY

M.A. Van Zeeland, RSI, 2008 *et al.*

Vibration compensation is required for a short CO2 wavelength in tokamaks

An alternative two-color method -dispersion interferometer (Homodyne tech.)

Using one CO_2 laser instead of two and frequency doubler to provide two-color lasers

Phase shift due to plasma:

$2\omega: \frac{c_p \overline{n}_e L}{2\omega} \quad \omega: \frac{c_p \overline{n}_e L}{\omega}$

Phase shift due to mechanical vibrations:

$2\omega: \frac{2\omega\Delta d}{c} \quad \omega: \frac{\omega\Delta d}{c}$

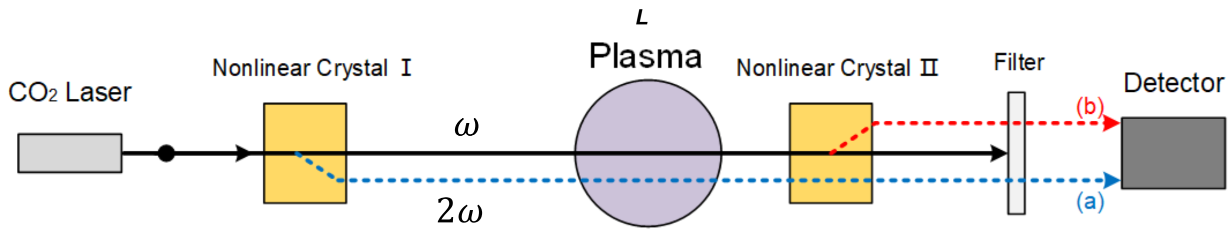

The phase of two second harmonic:

$$(a)\ \varphi_1 = 2\omega t + \frac{2\omega\Delta d}{c} + \frac{c_p \overline{n}_e L}{2\omega} + \phi_1$$

$$(b)\ \varphi_2 = 2\left(\omega t + \frac{\omega\Delta d}{c} + \frac{c_p \overline{n}_e L}{\omega} + \phi_2\right)$$

Interference signal of second harmonic:

$$I = A + B\cos(\varphi_1 - \varphi_2) = A + B\cos\left(\frac{3}{2}\frac{c_p \overline{n}_e L}{\omega} + \varphi\right) \Rightarrow \overline{n}_e = -\frac{2}{3}\frac{\omega}{c_p L}\left[\frac{\arccos(1-A)}{B} - \phi\right]$$

The mechanical vibration is perfectly cancelled out due to same optical path.

This is a homodyne system which requires stable amplitude of signals.

T. Akiyama, K. Kawahata, S. Okajima and K. Nakayama, Plasma and Fusion Research 5 (2010)S1041.

Toroidal CO_2 Dispersion Interferometer on EAST

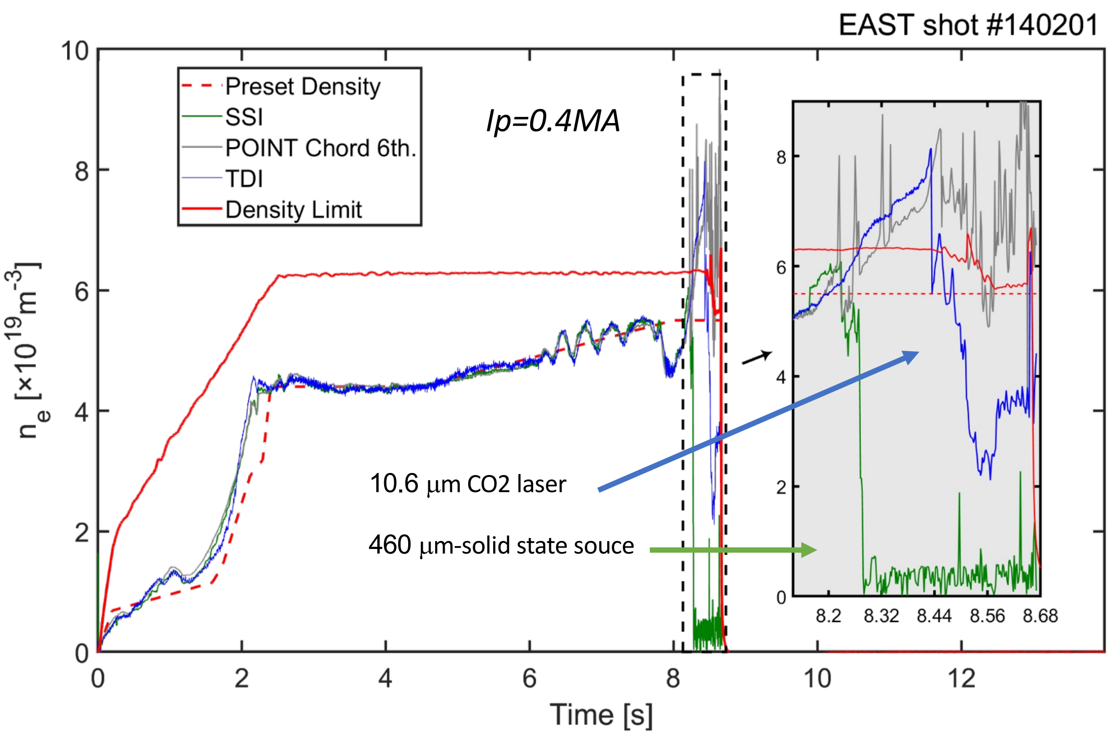

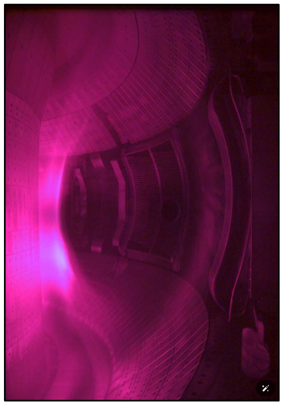

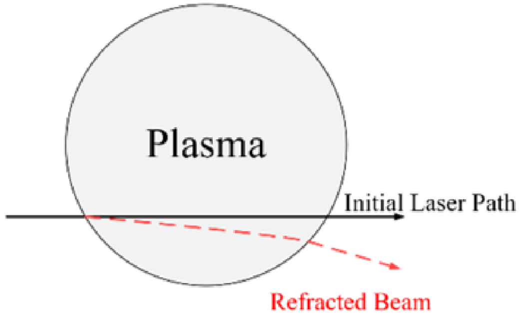

Toroidal Dispersion Interferometer can provide density feedback control near the density limit where Long wavelength beam might be deflected by large density gradient

(λ=461μ m) Interferometer (0.65THz solid state source) on KTX Reversed Field Pinch

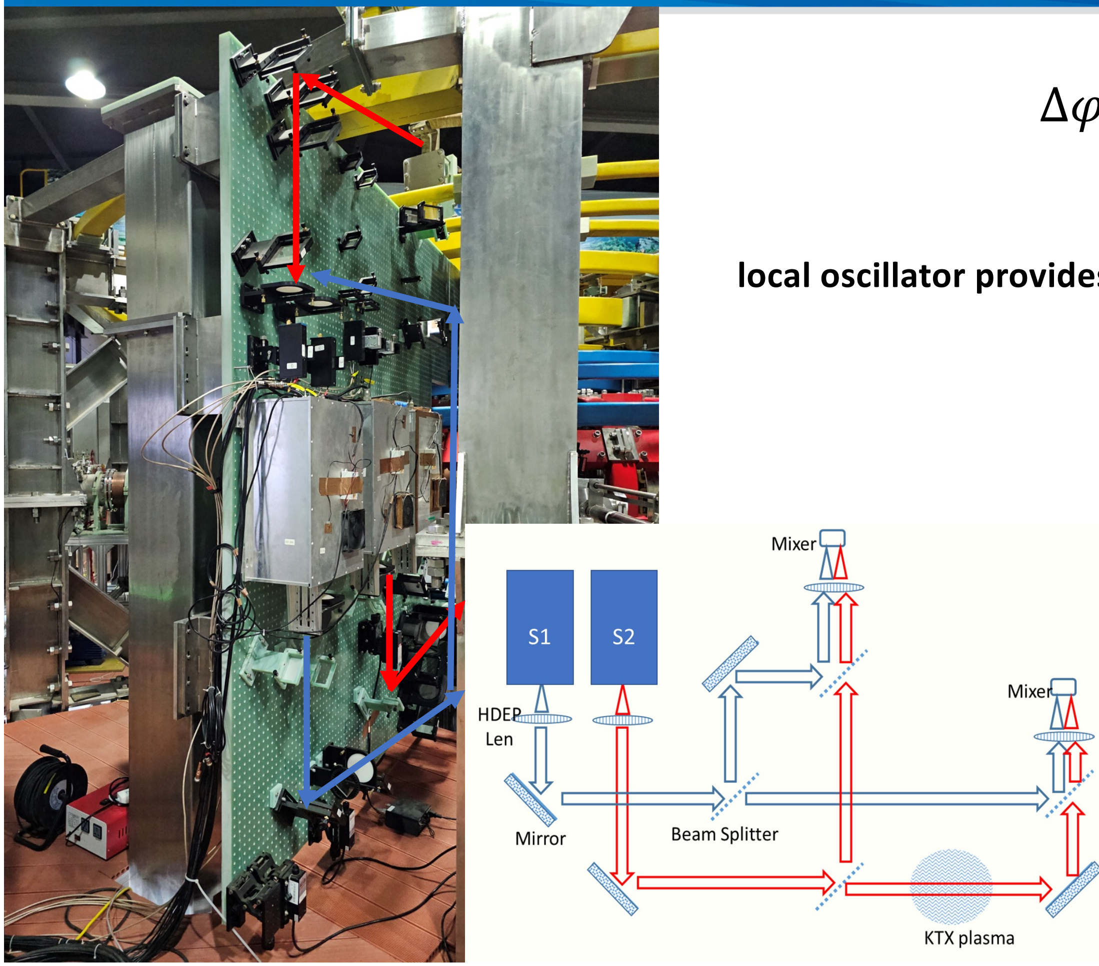

$$\Delta\varphi = 2.82\times10^{-15}\lambda\int n_e dl + \frac{2\pi}{\lambda}N_0\Delta l$$

No vibration Compensation *For long wavelength*

local oscillator provides a beat frequency (IF) for heterodyne measurement

$$I_1 = I_A + I_B\cos(\Delta\omega + \varphi) \quad \Delta\omega = \omega_1 - \omega_2 \ll \omega_{1,2}$$

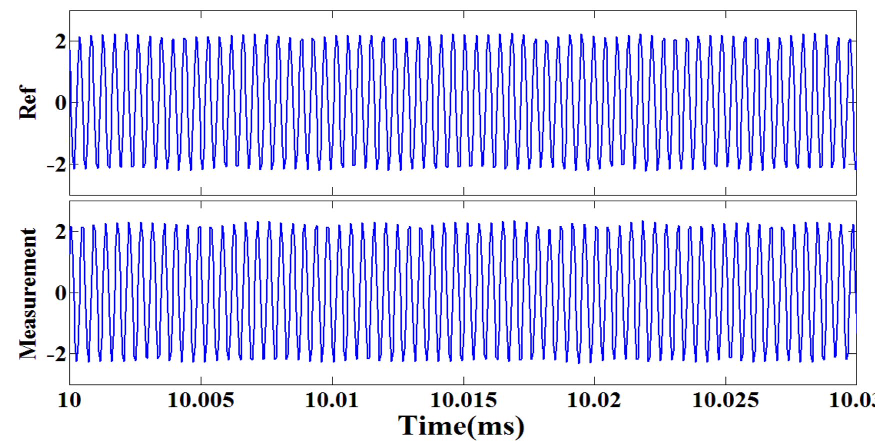

Five-chord Density Interferometer on KTX

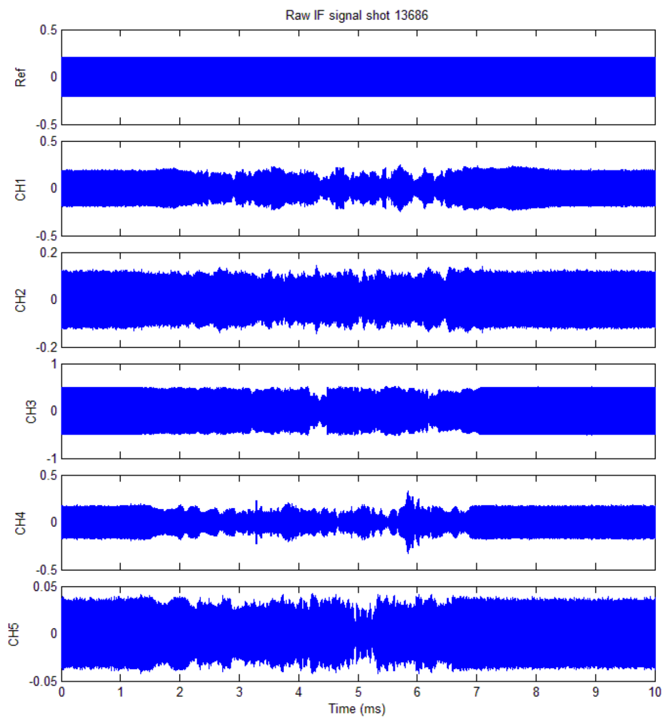

Amplitude of raw signals during plasma discharge

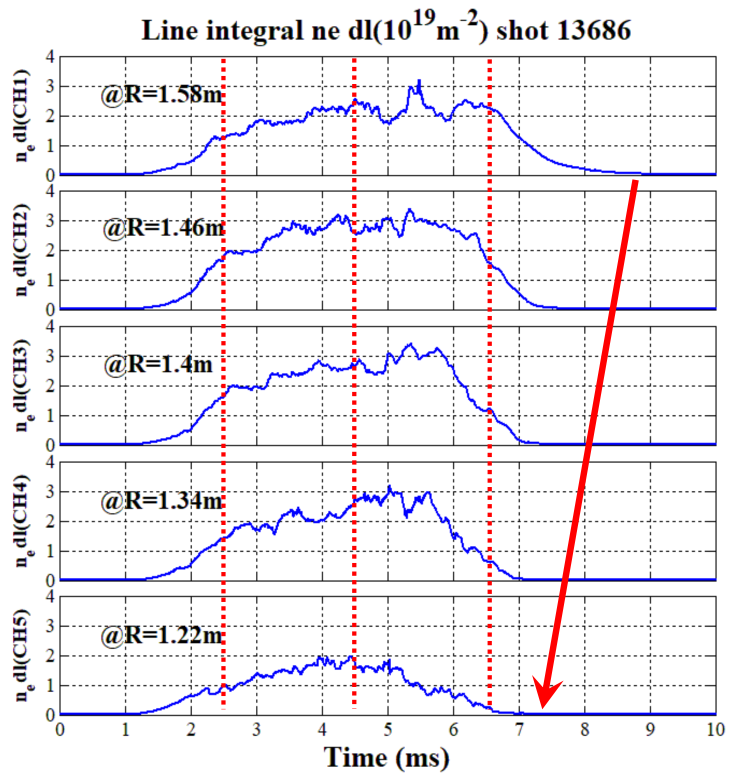

Time history of 5 chord line electric density from outside board to inside board

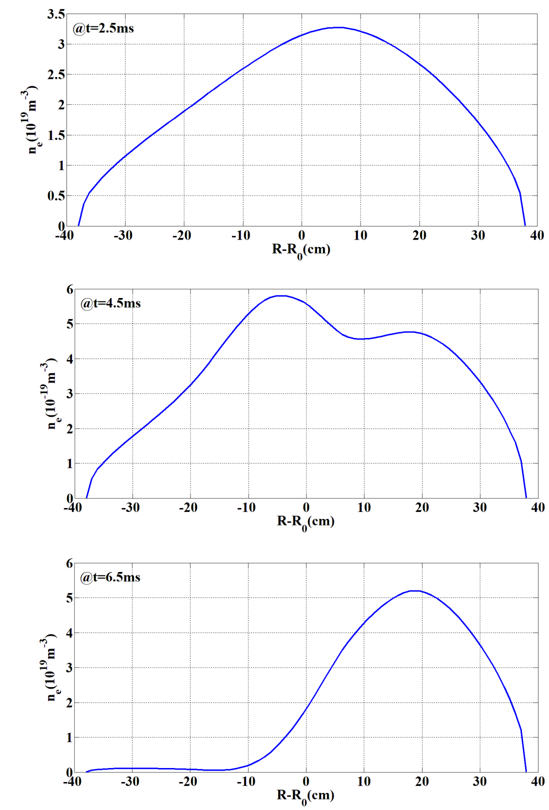

Evolution of electric density profiles

Polarimetry –
Faraday-effect Based Magnetic Field Measurement

Faraday Rotation Effect in Plasmas

The linearly polarized EM wave is equivalent to the superposition of L-wave and R-wave.

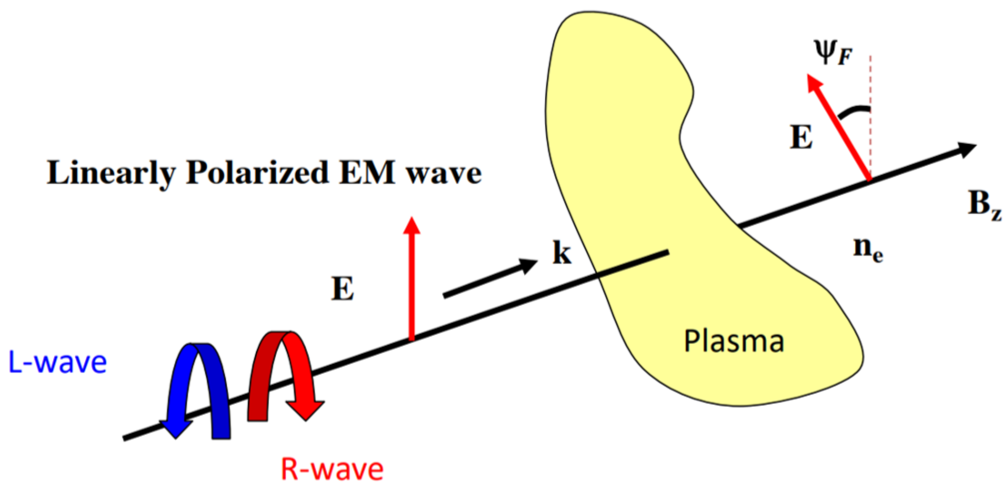

$$\varphi_L = \frac{2\pi}{\lambda}\int_{Z_1}^{Z_2} N_L dz \qquad N_L = 1 - \frac{1}{2}\frac{\omega_{pe}^2}{\omega^2}\left(1 - \frac{\omega_{ce}}{\omega}\right)$$

$$\varphi_R = \frac{2\pi}{\lambda}\int_{Z_1}^{Z_2} N_R dz \qquad N_R = 1 - \frac{1}{2}\frac{\omega_{pe}^2}{\omega^2}\left(1 + \frac{\omega_{ce}}{\omega}\right)$$

$$\left(\ \omega_{pe}^2 = \frac{n_e e^2}{m_e \varepsilon_0} \qquad \omega_{ce} = \frac{eB_z}{m_e} \qquad n_c = \frac{\omega^2 m_e \varepsilon_0}{e^2}\ \right)$$

$$\Psi_F = \frac{\varphi_L - \varphi_R}{2} = \frac{2\pi}{\lambda}\int_{Z_1}^{Z_2} \frac{N_L - N_R}{2} dz = \frac{e}{2cm_e n_c}\int_{Z_1}^{Z_2} n_e B_z dz \Rightarrow \Psi_F = 2.62\times10^{-13}\lambda^2 \int_{Z_1}^{Z_2} n_e B_z dz$$

The phase velocity of L-wave and R-wave is different， so there is a Faraday rotation angle Ψ_F between the linearly polarized incident wave and the emergent wave.

Two-wave Measurement Technique of Polarization

- R-waves and L-waves are offset in frequency

Dodel & Kunz, 1978

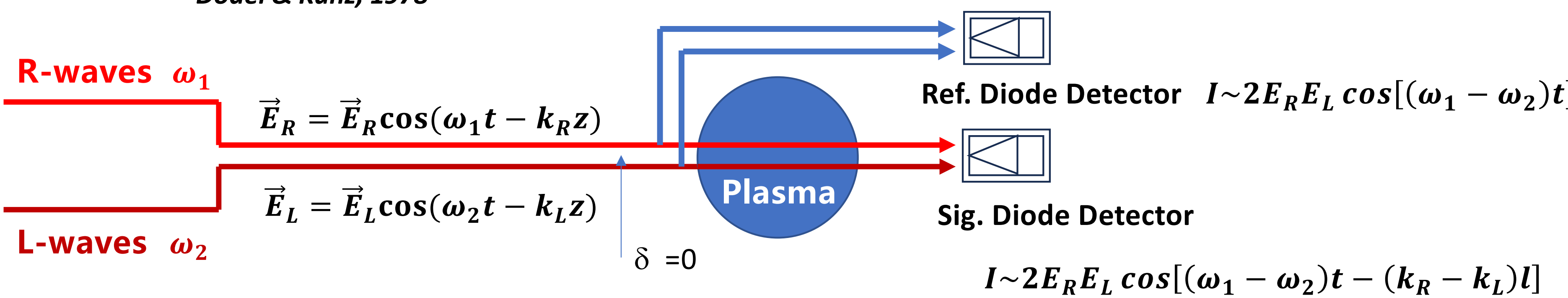

- the beat frequency signal: $|\omega_1-\omega_2| \rightarrow \Psi_F$

(Faraday effect Polarimeter)

$$\Psi_F = \frac{\varphi_L-\varphi_R}{2} \qquad \left(\frac{N_L-N_R}{2} = \frac{1}{2}\frac{\omega_{pe}^2}{\omega^2}\frac{\omega_{ce}}{\omega}\right)$$

$$\Psi_F = 2.62\times10^{-13}\lambda^2\int_{Z_1}^{Z_2} n_e B_z dz$$

(Cotton-Mouton Effect Polarimeter)

$$N_o - N_x = \frac{1}{2}\frac{\omega_{pe}^2}{\omega^2}\frac{\omega_{ce}^2}{\omega^2}$$

$$\phi_{CM}\,[\mathrm{rad.}] = \phi_O - \phi_X$$
$$= 2.4\times10^{-20}\,\lambda[\mathrm{mm}]^3\int n_e[\mathrm{m}^{-3}]\,B_\perp[\mathrm{T}]^2\,dl[\mathrm{m}]$$

MIT C-mod Laser Faraday effect Polarimetry (λ =117μm)

- **Two CW far infrared lasers(FIR) (Cohere Inc.: λ=117 μm, 150 mW/cavity).**
- **Frequency offset 4 MHz (<1 ms time response)**
- **~14 m pathlength, double path system-retro-reflector is used to return beams back to detectors.**

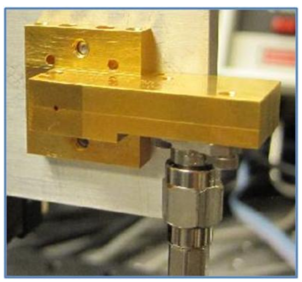

VDI planar Diode

W. F. Bergerson, P. Xu, J. H. Irby, D. L. Brower, W. X. Ding, and E. S. Marmar, RSI, 2012

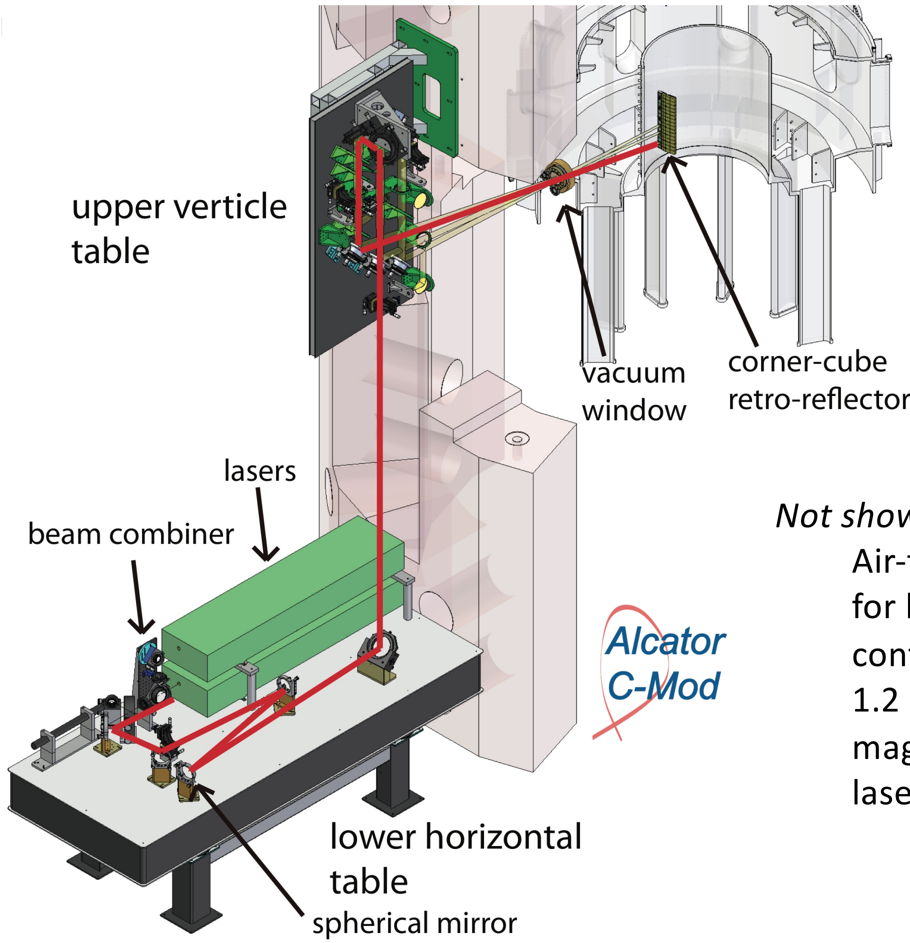

C-Mod Parameters:

B_T = 3 - 8T

Ip = .4 - 2.1MA

ne **= 0.3 - 5.0x10 ^{20}m-3**

R = 0.68 m

a = 0.22 m

Not shown:

Air-tight enclosures for humidity control

1.2 cm thick magnetic shield for laser stability

Faraday Effect used to constrain magnetic equilibrium reconstruction to obtain current profile

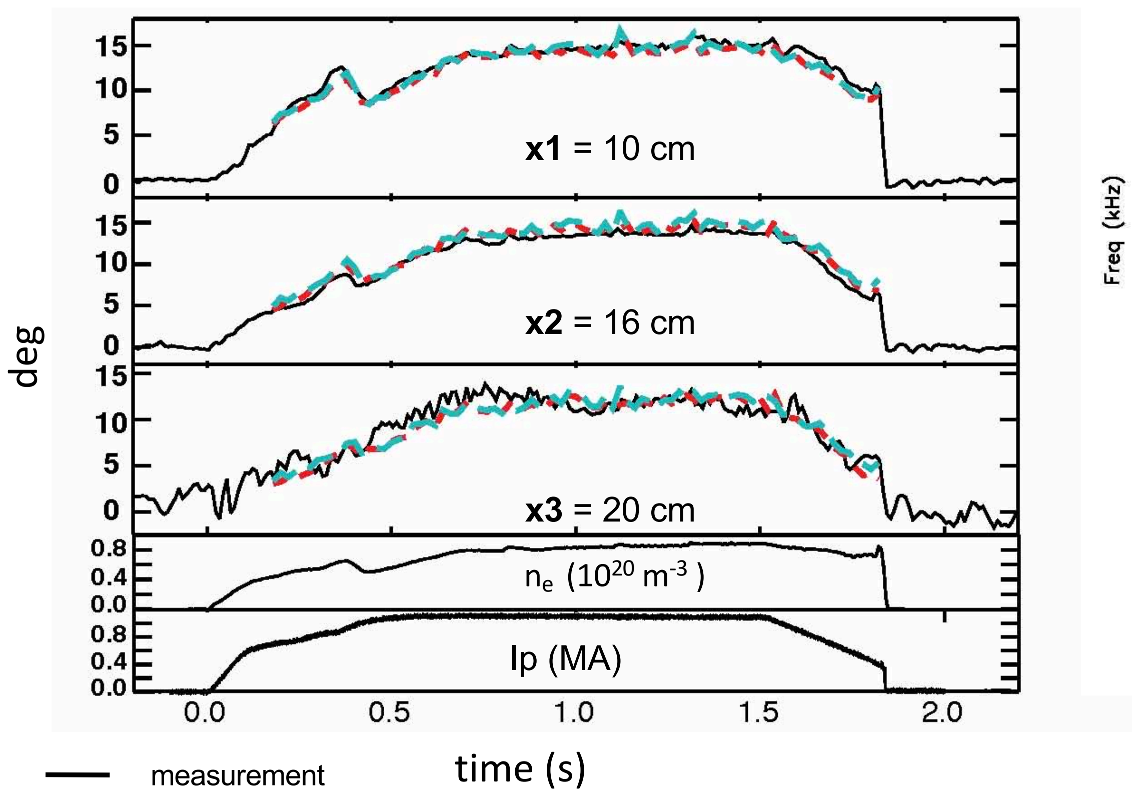

- Experiment and EFIT agree

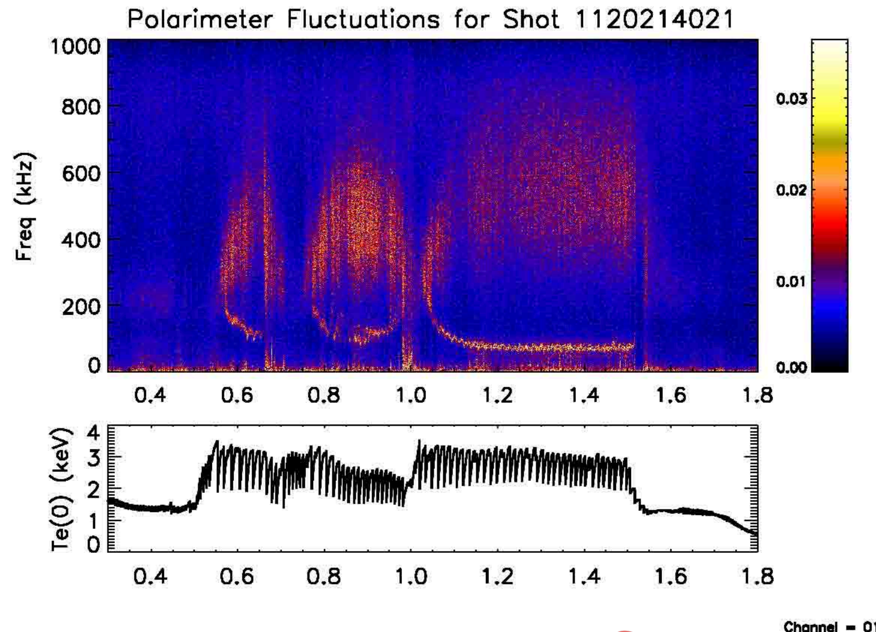

UCLA

Alcator C-Mod

C-Mod polarimeter has time and phase resolution not only for equilibrium but also fluctuation measurements!

Cotton-Mouton Effect Polarimeter on C-Mod

Instead R and L waves, ***Probing plasma with linear orthogonal light***

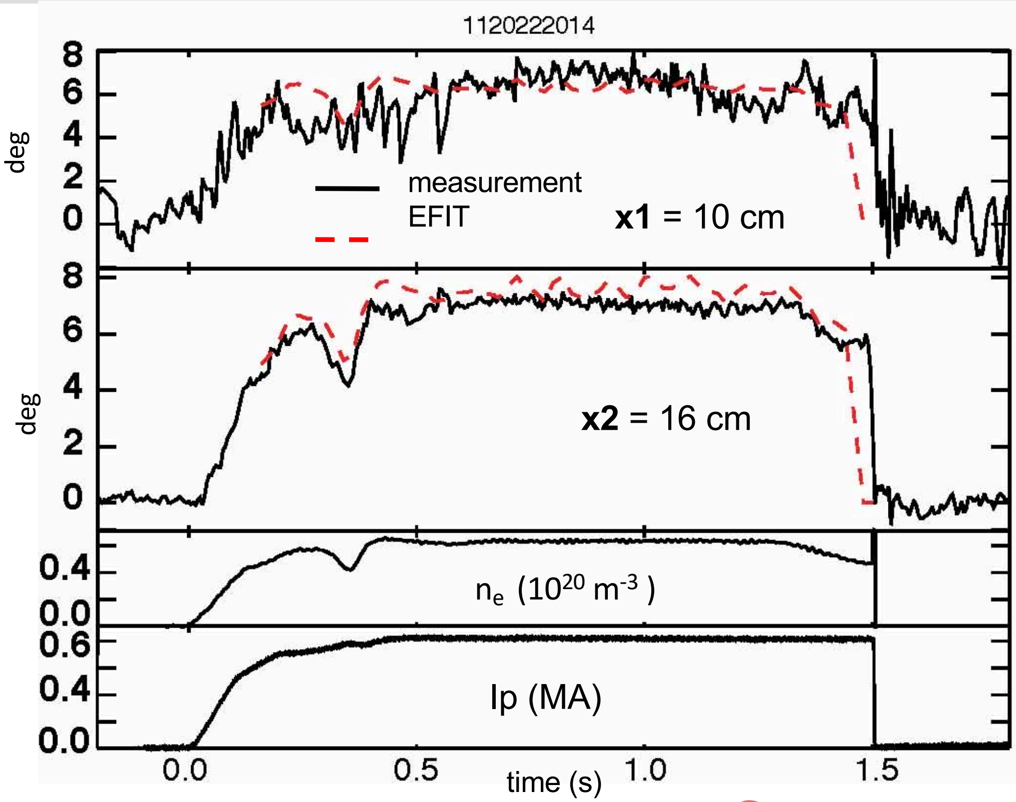

1) Cotton-Mouton and Faraday effect measurements consistent with EFIT
2) C-M effect can be used to measure density as B_T is known

$$\phi_{CM}\,[\text{rad.}] = \phi_O - \phi_X$$
$$= 2.4\times10^{-20}\,\lambda[\text{mm}]^3 \int n_e[\text{m}^{-3}]\,B_\perp[\text{T}]^2\,dl[\text{m}]$$

UCLA Alcator C-Mod

Three-wave Measurement Technique of Polarization (LO beam added)

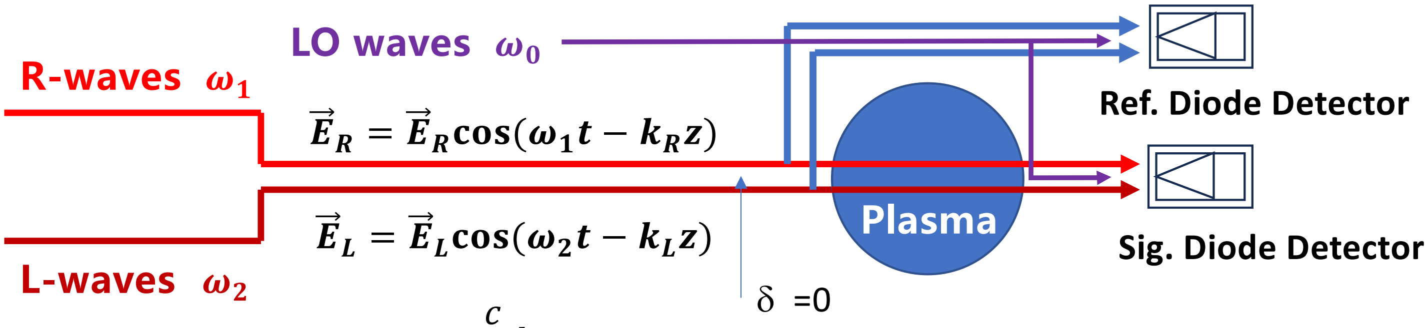

$$\vec{E}_R = \vec{E}_R \cos(\omega_1 t - k_R z)$$

$$\vec{E}_L = \vec{E}_L \cos(\omega_2 t - k_L z)$$

$$N = \frac{c}{\omega} k$$

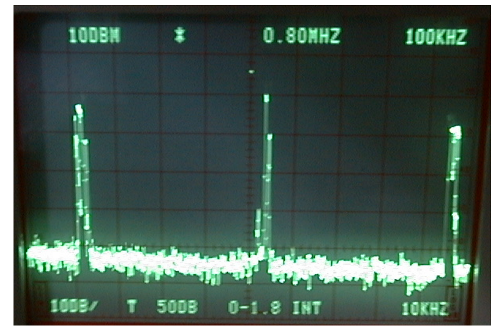

$$I = 2E_R E_L \cos[(\omega_1 - \omega_2)t - (k_R - k_L)l] + E_R E_{LO} \cos[(\omega_1 - \omega_0)t - k_R l] + E_L E_{LO} \cos[(\omega_2 - \omega_0)t - k_L l]$$

Rommers & Howard, 1996
Ding et al., 2003

Faraday rotation angle

$$\Psi_F = \frac{\varphi_L - \varphi_R}{2} \qquad \left(\frac{N_L - N_R}{2} = \frac{1}{2}\frac{\omega_{pe}^2}{\omega^2}\frac{\omega_{ce}}{\omega} \right)$$

$$\Psi_F = 2.62 \times 10^{-13} \lambda^2 \int_{Z_1}^{Z_2} n_e B_z dz$$

$$\Delta\varphi = \frac{\varphi_L + \varphi_R}{2} \qquad \left(\frac{N_L + N_R}{2} = 1 - \frac{1}{2}\frac{\omega_{pe}^2}{\omega^2} \right)$$

$$\Delta\varphi = 2.82 \times 10^{-15} \lambda \int n_e dl$$

POlarimetry-INTerferometer (POINT) on EAST

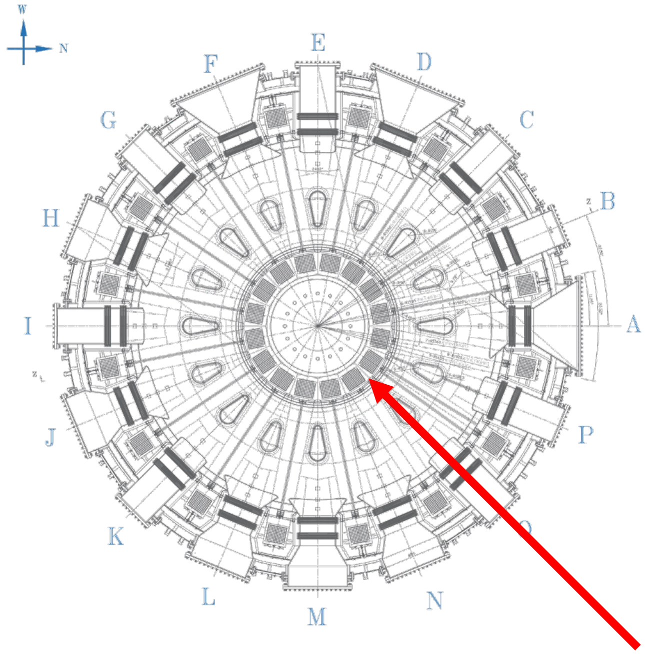

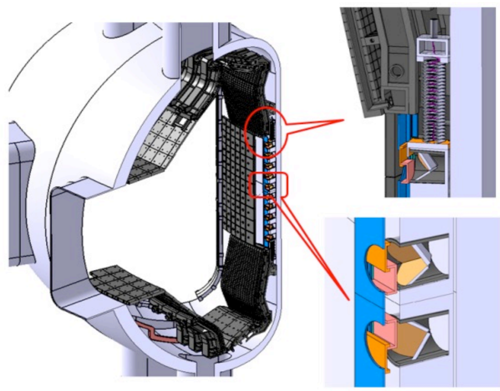

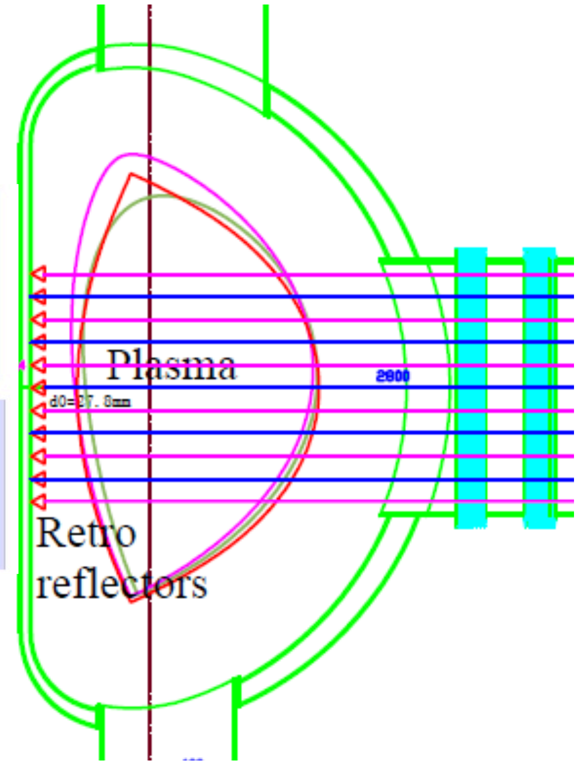

Laser Beams (λ =432μ m)

- **Horizontal measurement** **11chords** **(space resolution:** **8.5cm****)**
- **Time resolution:** **1μs**

Three wave technique-simultaneous measurements of density and magnetic field

Digital Phase Demodulator for Three Wave System

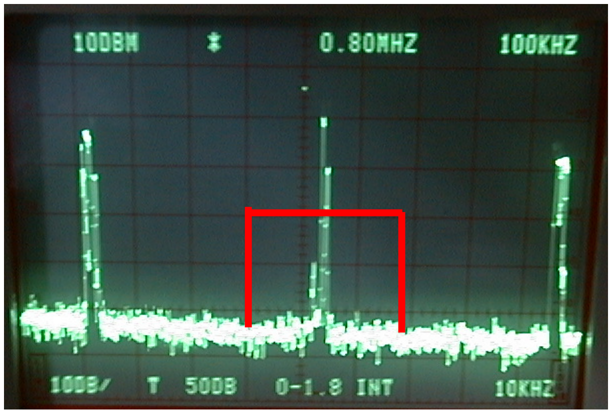

$$I\_sig = 2E_RE_L\cos[(\omega_1-\omega_2)t-(k_R-k_L)l]$$
$$+E_RE_{LO}\cos[(\omega_1-\omega_0)t-k_Rl]$$
$$+E_LE_{LO}\cos[(\omega_2-\omega_0)t-k_Ll]$$

$$I\_ref = 2E_RE_L\cos[(\omega_1-\omega_2)t]$$
$$+E_RE_{LO}\cos[(\omega_1-\omega_0)t]$$
$$+E_LE_{LO}\cos[(\omega_2-\omega_0)t]$$

I_sig
I_ref → FFT, Select Bandwidth Filter

$$I\_sig = A\exp(i[(\omega_1-\omega_2)t-(k_R-k_L)l])$$
$$I\_ref = B\exp(i[(\omega_1-\omega_2)t])$$

Demodulate

$$(k_R-k_L)l = \arctan\frac{Im(I_{sig}I^*_{ref})}{Re(I_{sig}I^*_{ref})}$$

Y.Jiang, et al. RSI, 1997

Real-time calculate density and Faraday rotation angle,Output: 250 kS/s . ***Palomar Scientific Instruments,***

A Long Pulse Discharge 100s on EAST

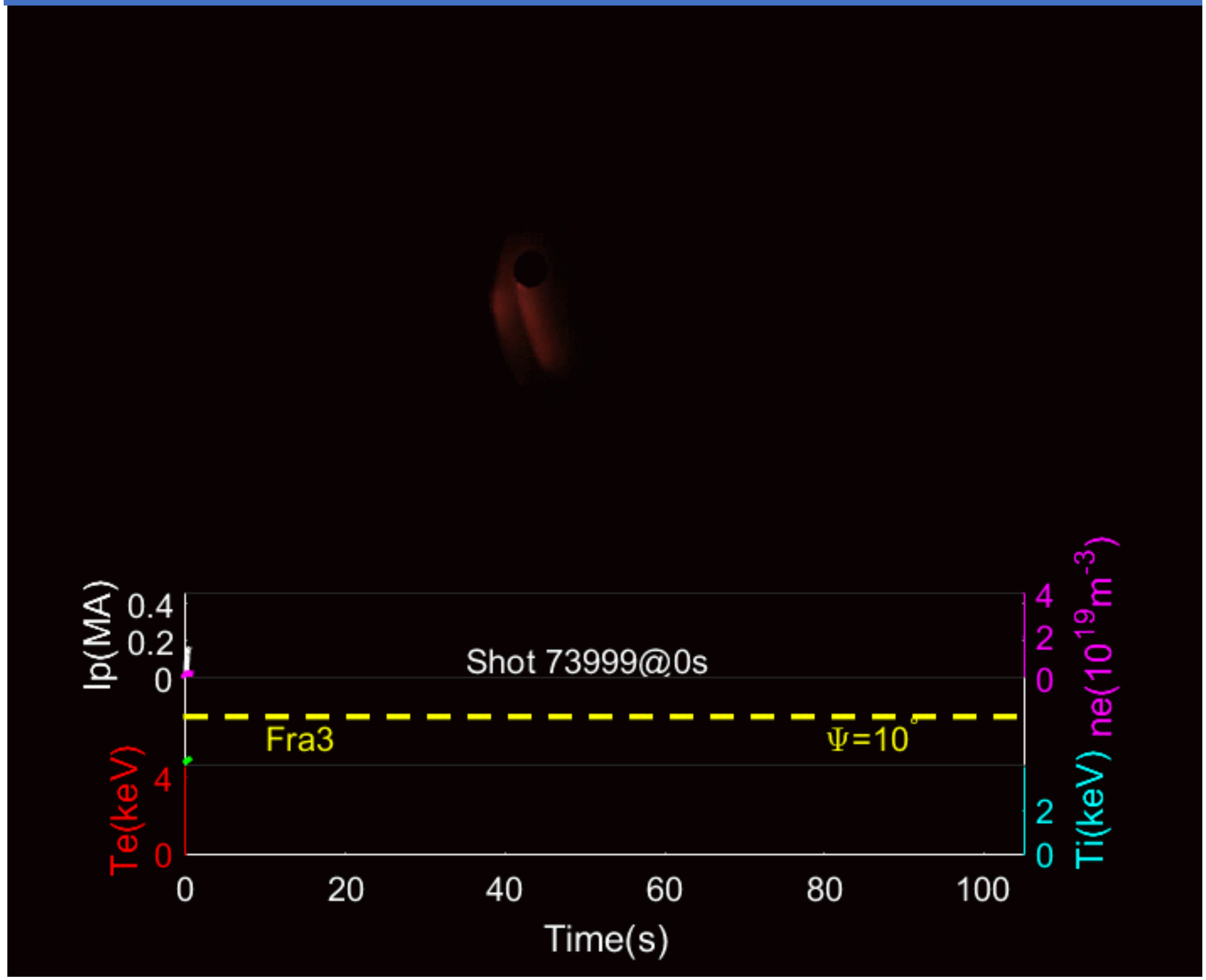

Real-time density and Faraday rotation angle

Current profile Measurement with constrains from Faraday effect polarimetry

Time history of 11-chord density and Faraday rotation

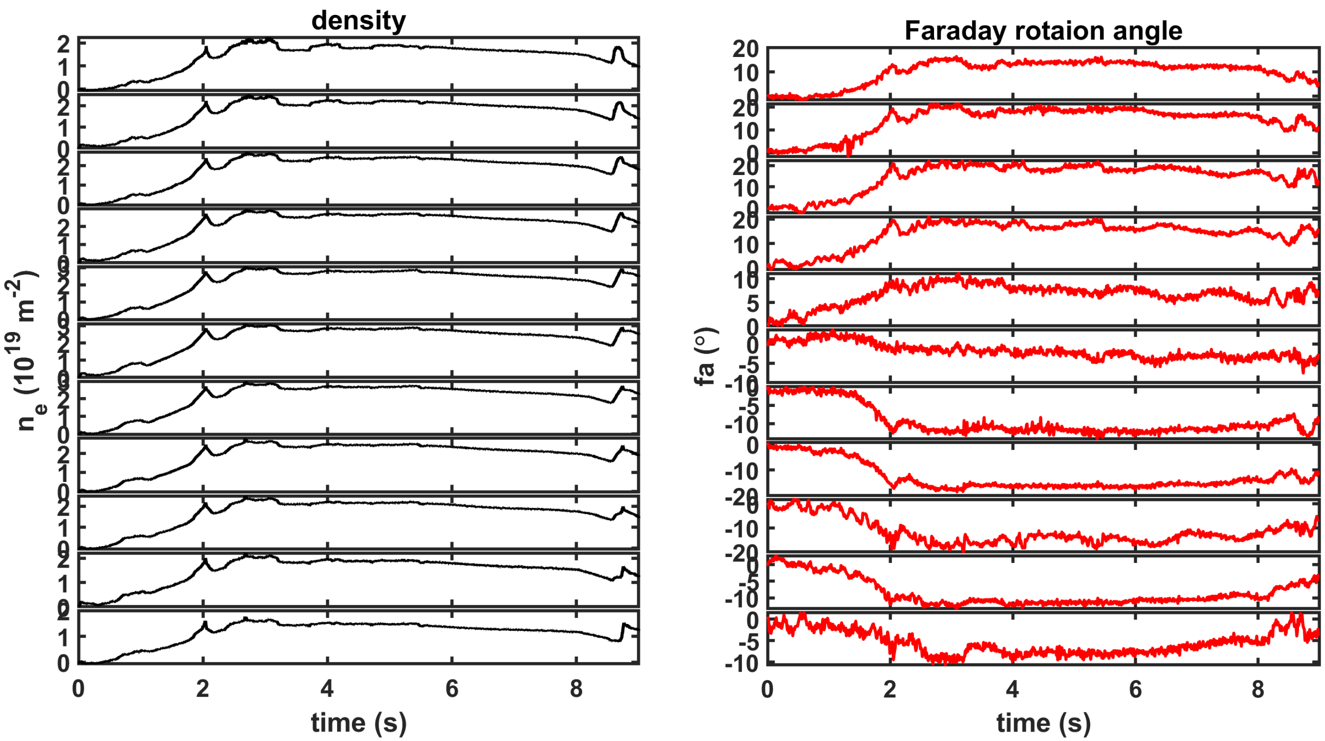

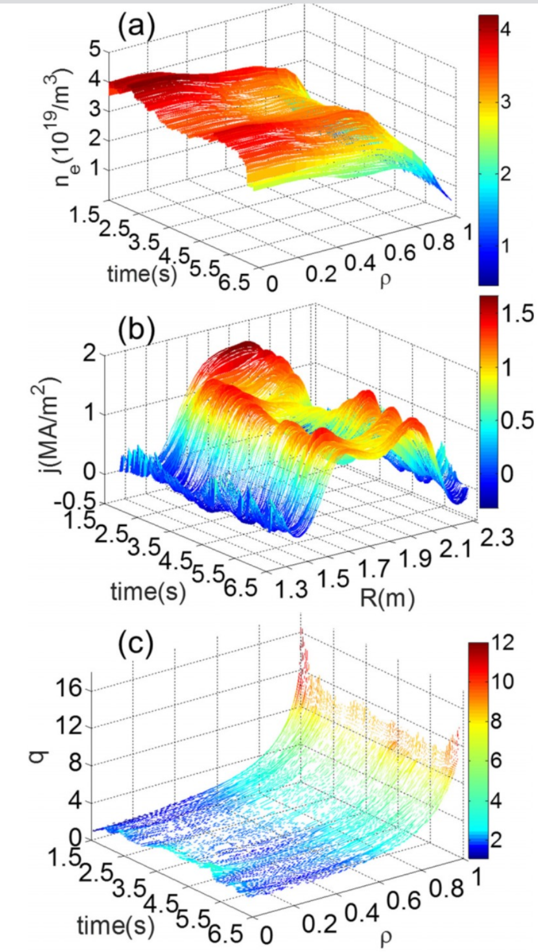

Faraday effect polarimetry provides current profile for fusion plasmas with fast time response!

Polarimeter can be used for density measurement on ITER

Polarimetry can be density measurement while toroidal magnetic field B_T is known.

- Interferometer phase shifts >> 360°
  - Need to count "fringes" (1 fringe = 360°)
  - Signal loss ➔ Loss of fringe count ➔ loss of measurement

$$\int n_e dL = \frac{\lambda_{CO2}}{r_e(\lambda_{CO2}^2 - \lambda_{QCL}^2)}\left[\phi_{CO2} - \frac{\lambda_{QCL}}{\lambda_{CO2}}\phi_{QCL}\right]$$

- Polarimetry measures Faraday rotation phase shifts < 360°
  - No need to count fringes
  - Used to correct interferometer after a fringe skip
  - Also provides backup density measurement

$$\Psi_F = 2.62\times10^{-13}\lambda^2\int n_e B_z dl$$

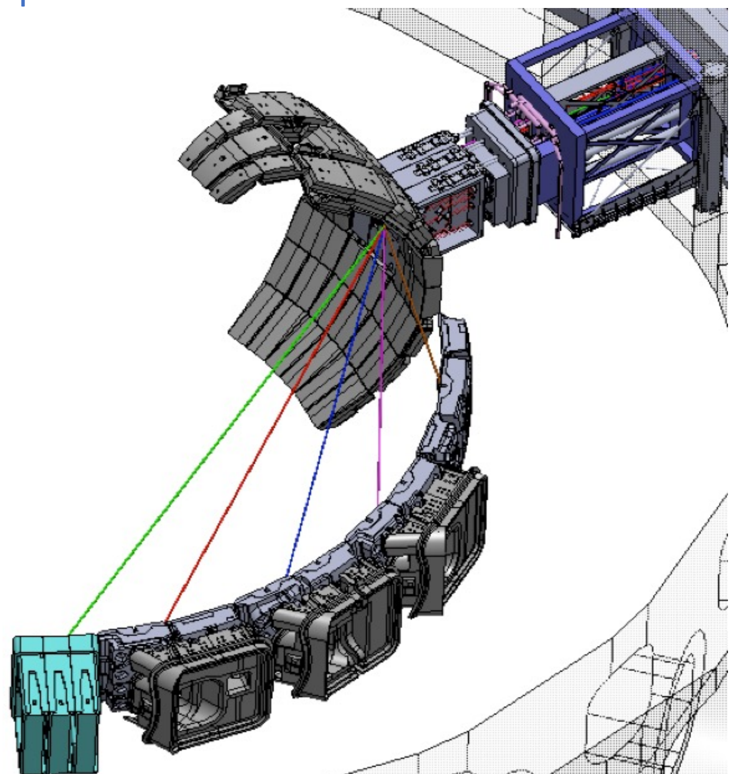

Fringes count errors are NOT allowed for plasmas control!!

Two-Color Interferometer + Faraday effect Polarimetry for ITER Density Control

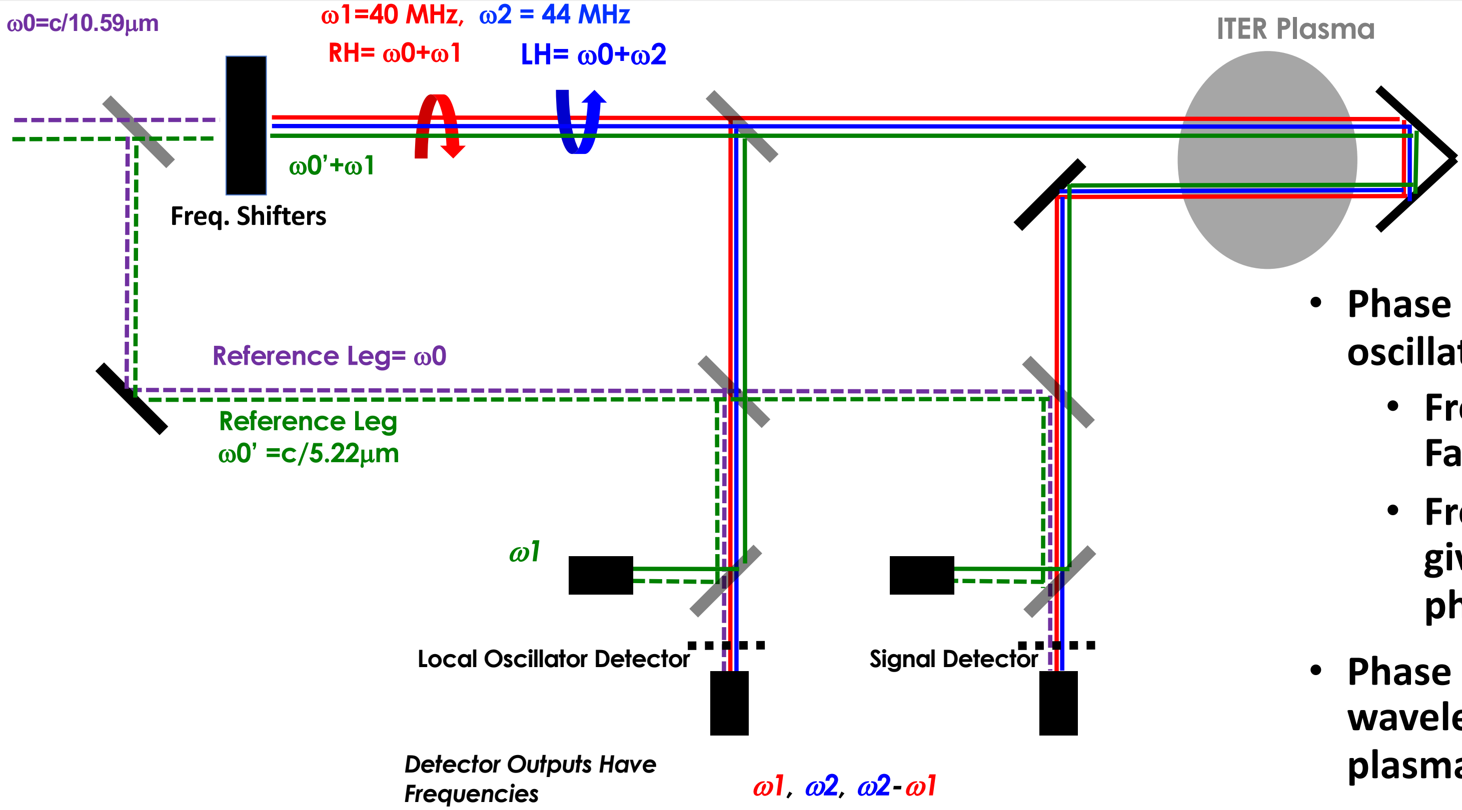

- Phase of signal detector vs. local oscillator detector at:
  - Frequency $(\omega_2 - \omega_1)$ will give 2X Faraday rotation
  - Frequency ω_1 and/or ω_2 will give *plasma + vibration* induced phase shift
- Phase difference at ω_1 of shorter wavelength allows separation of plasma and vibration phase shifts

Add one more probing beam (L, R wave now) into two-color interferometer , providing Faraday rotation measurements

Polarimeter corrects fringe skip of interferometer

- **Interferometer phase shifts >> 360 degree , history dependence, loss signals and loss history.**
  - Need to count "fringes" (1 fringe = 360^{O})
  - Signal loss ➔ Loss of fringe count ➔ loss of measurement
- **Polarimeter phase is less than 1 fringe so absolute phase is recovered when signal returns**
- **Polarimeter can be used to recalibrate the interferometer**

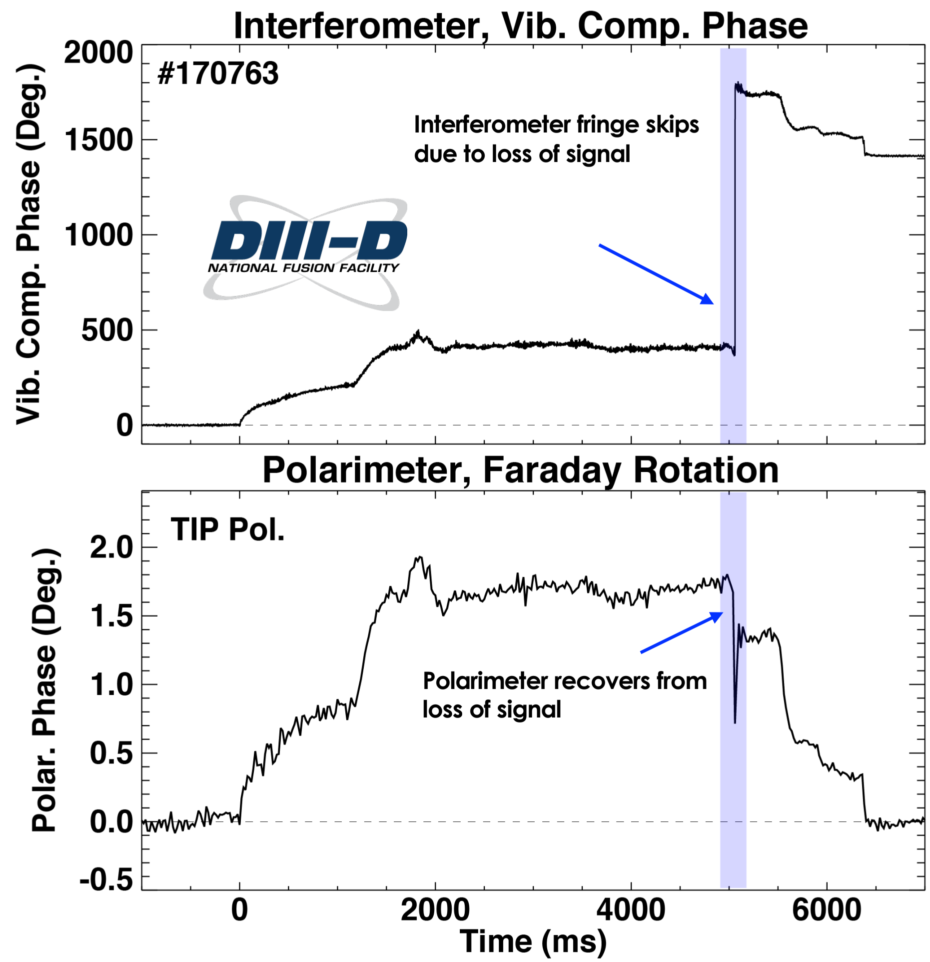

Interferometer is still needed for its better density resolution; Polarimeter helps to correct fringe skip in case to ensure the relaibility of density measurement for fusion reactor.

PoPola –Polarimetry on ITER

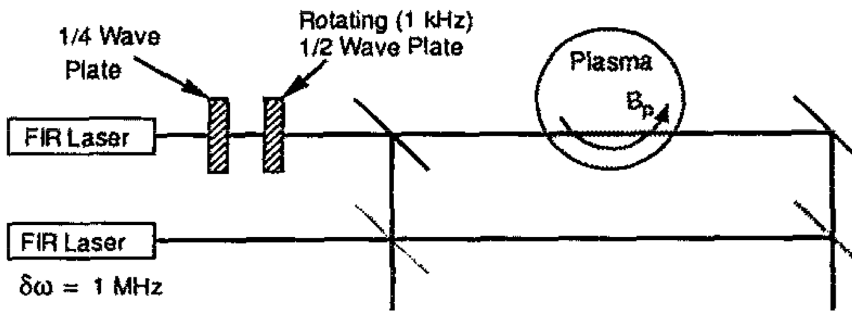

B.W.Rice, et al. RSI, (1992). H.Soltwisch, RSI. 1986

- **13 laser probing beams at wavelength $119\mu m$ (a few hundred mW) ;**
- **Faraday rotation and Cotton-Mouton effects are measured to reconstruction of current profile;**
- **Polarization modulation by mechanical rotation (~ a few hundred Hz) of a waveplate.**

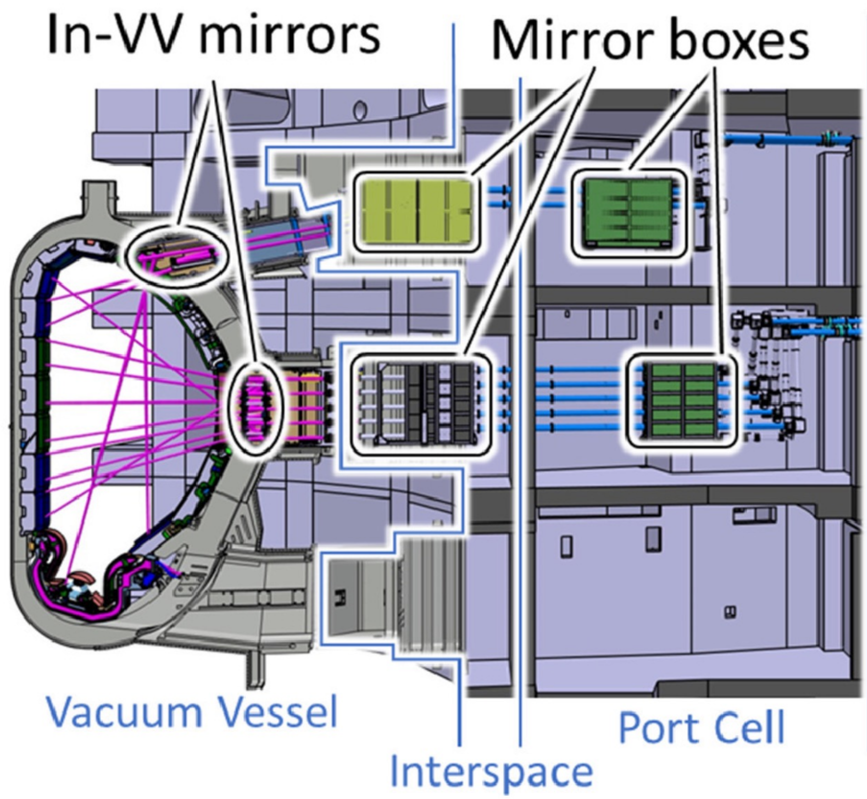

R. Imazawa, *et al* Fusion Eng. Design, 2023

Application of line integrated Faraday rotation to plasma vertical position measurement

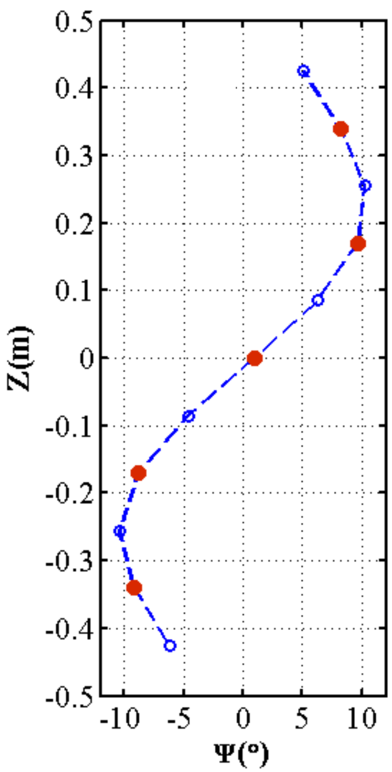

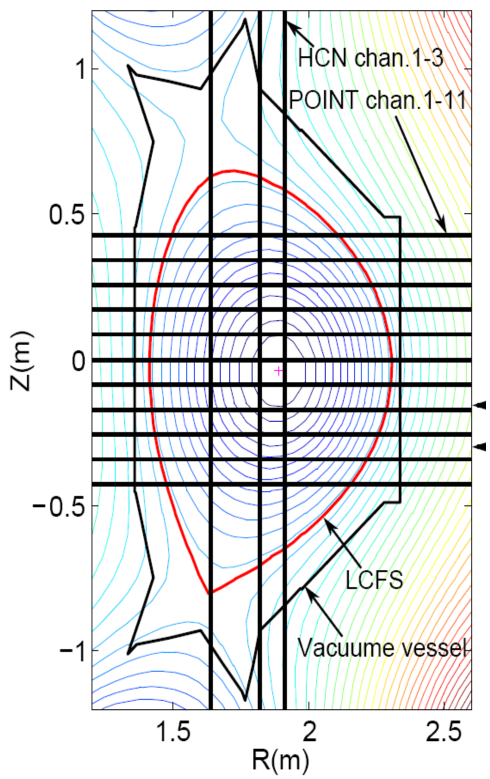

$$\Psi = c_p \int n_e(R,Z) B_R(R,Z) dR$$

$$B_R(R,Z_c)=0$$

Determine Z where

$$\Psi(\mathrm{R,Z})=\Psi(Z_0)+(Z-Z_0)\frac{\partial\Psi}{\partial Z}+\cdots=0$$

$$Z_F=\frac{\Psi(0)}{-\frac{\partial\Psi(0)}{\partial z}}$$

Direct using line-integrated Faraday rotation data to determine the vertical position of plasmas

W.X.Ding, H.Q.Liu, et al. Rew. Sci.Instrum. Vol.89,2018

Vertical Position Measurement by Using Three Central Chords

400kA Plasma

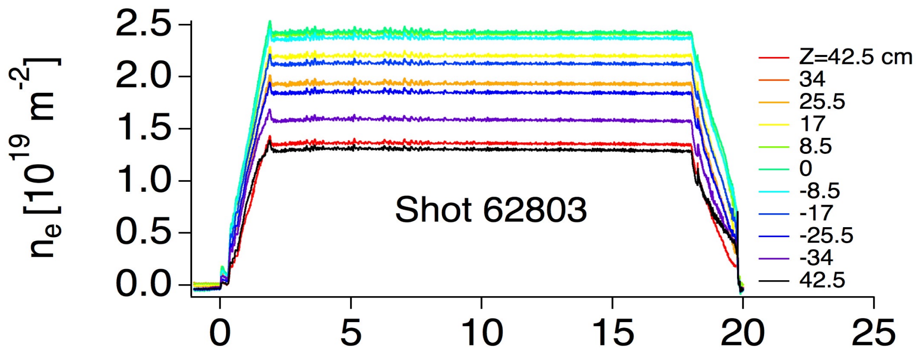

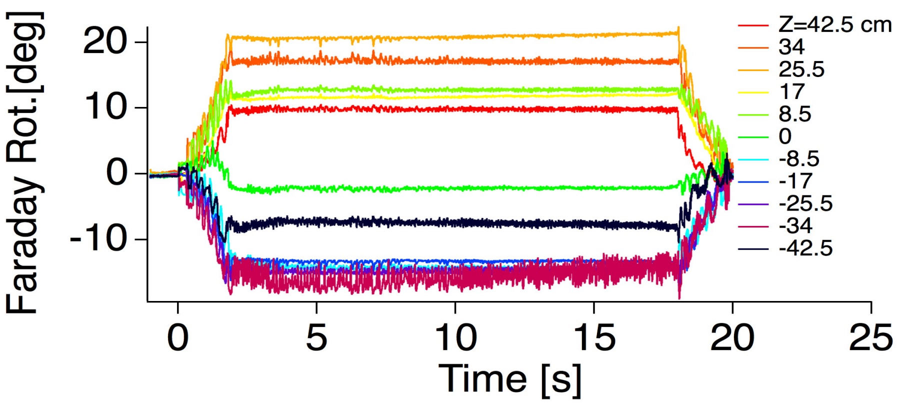

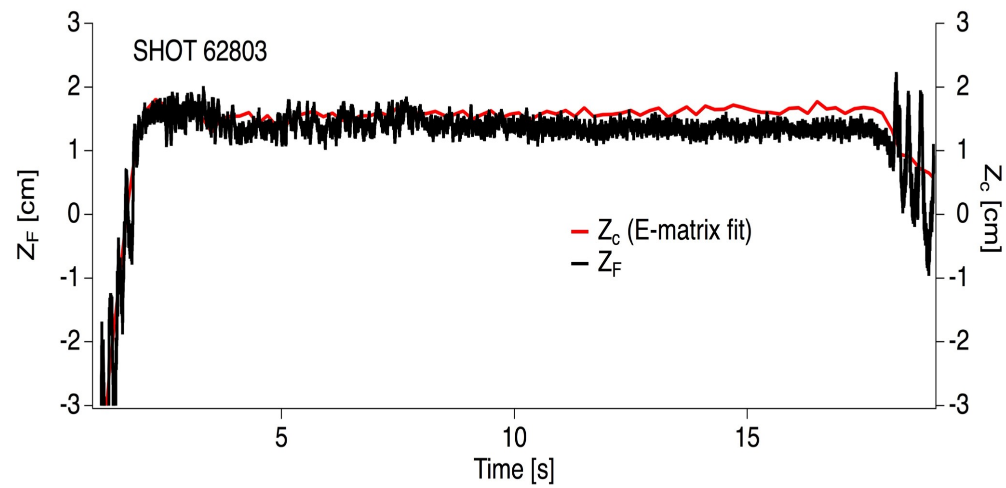

$$Z_F = \frac{\Psi(0)}{-\frac{\partial \Psi(0)}{\partial z}}$$

Non-inductive Polarimetry result is consistent with the measurements using flux loops as expected

Part III. (a) Dispersion Relation for Hot Plasmas

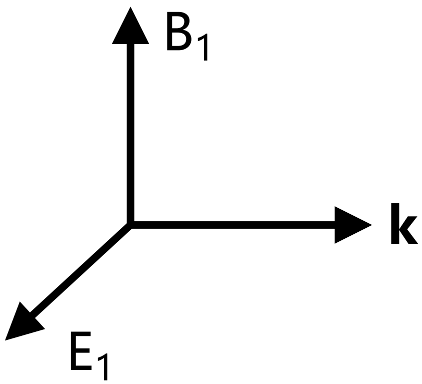

$$\nabla \times E_1 = -\frac{\partial B_1}{\partial t}$$

$$c^2 \nabla \times B_1 = \frac{\partial E_1}{\partial t} + j_1/\varepsilon_0$$

~~$j_1 = -e n_e v_{e1}$~~ Cold plasmas

$$\boldsymbol{j_1} = \boldsymbol{j_+} + \boldsymbol{j_-} = \frac{\boldsymbol{ie^2}}{\boldsymbol{m_e\gamma}}\left(\frac{\mathbf{1}}{\boldsymbol{\omega - kv}} + \frac{\mathbf{1}}{\boldsymbol{\omega + kv}}\right)\boldsymbol{E_1}$$

Doppler shift-Electrons move in two directions

$$\approx \frac{\boldsymbol{2ie^2}}{\boldsymbol{m_e\gamma\omega}}\left(\mathbf{1} + \frac{\boldsymbol{k^2v^2}}{\boldsymbol{\omega^2}}\right)\boldsymbol{E_1}$$

$\gamma = (1 - \frac{v^2}{c^2})^{-1/2}$ Relativistic factor

$f(p) \sim \exp(-\frac{p^2}{2m_e\gamma kT_e})$

In hot plasmas, Doppler shift of the frequency kv and change of electron mass both contribute to refractivity. Electron pressure is not perturbed for transverse mode.

V.V. Mirnov , W.X.Ding, D.L Brower et al., PoP, 2007

Relativistic effect must be included for interfrometer and polarimetry for finite temperature plasmas.

Non-relativistic and weakly relativistic thermal effects contribute with opposite sign

- **Overall increase of the refractive index N^2 due to relativistic γ - factor**

$$N^2 = \underbrace{1 - \frac{\omega_{pe}^2}{\omega^2}}_{\text{cold plasma}} - \frac{\omega_{pe}^2}{\omega^2}\underbrace{\left(\frac{T_e}{m_e c^2} - \frac{5T_e}{2m_e c^2}\right)}_{\text{combined model}}, \ +5\% \rightarrow -7.5\%, \ T_e = 25keV$$

non-relativistic

- **Relativistic corrections are larger than Doppler shift terms for interferometry and Faraday-effect polarimetry**

a) earlier non-relativistic model predicted increase of Ψ_F with Te

$$\Delta\Psi_F^{(NR)}/\Psi_F^{(c)} = 3(T_e/m_e c^2) \simeq +15\%$$

(S. Segre, V. Zanza, PoP, 2002)
Introduction to Plasma Physics and Controlled Fusion F.F. Chen

b) later relativistic calculations resulted in the opposite sign

$$\Delta\Psi_F^{(R)}/\Psi_F^{(c)} = -2(T_e/m_e c^2) \simeq -10\%$$

(V.V. Mirnov et al., PoP, 2007)

- **Reduction of the Doppler shift correction for the Cotton-Mouton effect (+60% $\rightarrow$ + 22.5%)**

Experimental Evidence of the weakly relativistic model on JET

Difference between induced ellipticity measured on JET and calculated from the cold plasma model $\chi - \chi_c$ plotted versus B_T^2 $\int$ Te ne dz *(O.P. Ford et al., PPCF, 2009)*

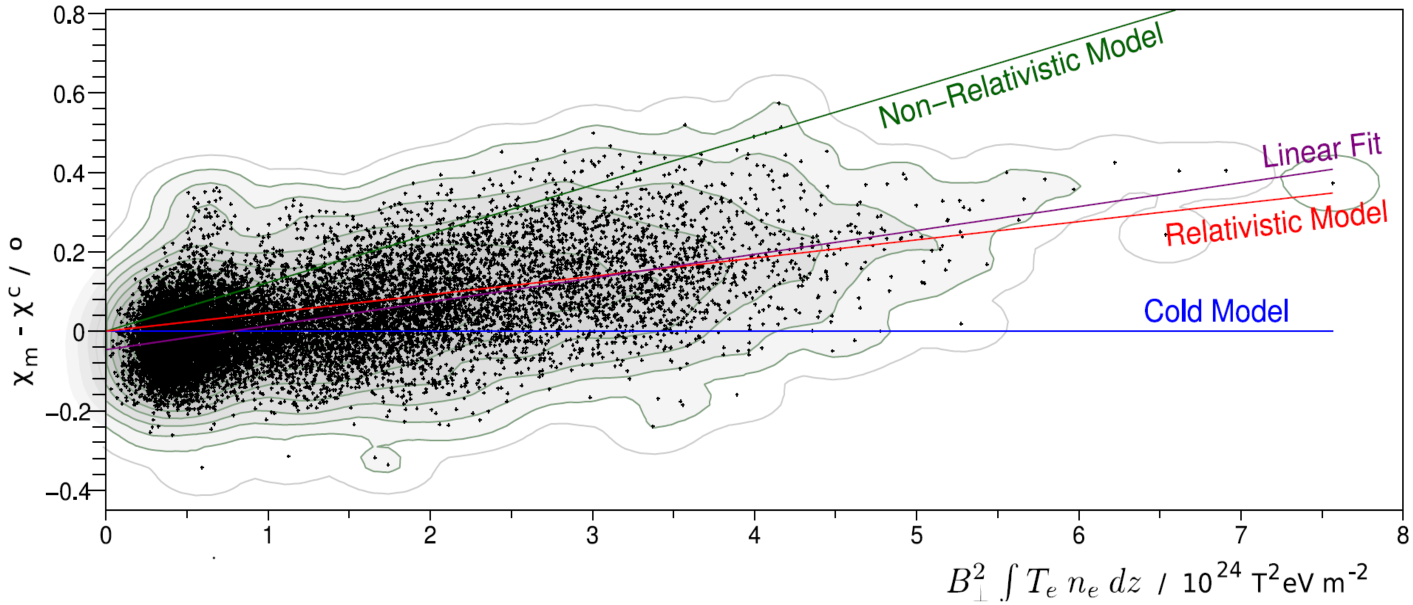

Solid lines illustrate cold plasma, non-relativistic and relativistic models (good agreement with the relativistic calculations)

First observation of the relativistic effects in plasma polarimetry

Part III: (b) Coupling between Cotton-Mouton and Faraday Rotation

In tokamaks, there are perpendicular magnetic fields along probing laser due to magnetic shear

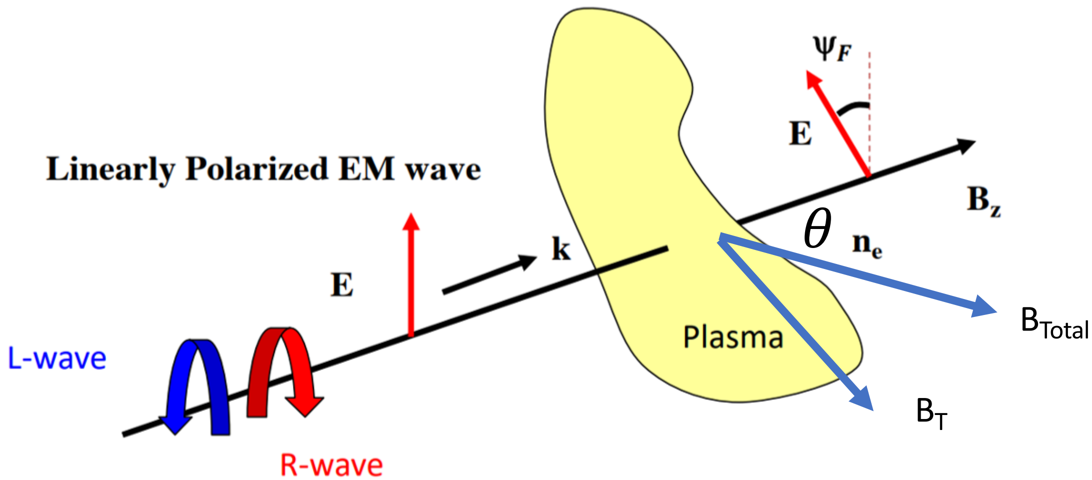

$$\varphi_{\mathrm{FR}} = 2.63 \times 10^{-13}\lambda^2 \int n_e B_{\parallel} \mathrm{d}l$$

$$\varphi_{\mathrm{CM}} = 2.46 \times 10^{-11}\lambda^3 \int n_e B_{\perp}^2 \mathrm{d}l$$

Perpendicular Magnetic Field may impact Faraday rotation measurements

$$N_{\pm}^2 = 1 - \frac{\omega_{pe}^2/\omega^2}{1 - \frac{\omega_{ce}^2/\omega^2 \sin^2\theta}{2\left(1-\frac{\omega_{pe}^2}{\omega^2}\right)} \pm \left[\frac{\omega_{ce}^4/\omega^4 \sin^4\theta}{4\left(1-\frac{\omega_{pe}^2}{\omega^2}\right)^2} + \frac{\omega_{ce}^2}{\omega^2}\cos^2\theta\right]^{1/2}}$$

Appleton-Hartree formula

$$E^+ = \begin{pmatrix} 1 \\ -i/\alpha \end{pmatrix} \exp(i(\omega t - k_+ z))$$

$$E^- = \begin{pmatrix} 1 \\ i/\alpha \end{pmatrix} \exp(i(\omega t - k_- z))$$

$$\alpha = \frac{(\omega_{ce}/\omega)\sin^2\theta}{2(1-\omega_{pe}^2/\omega^2)\cos\theta} - \left[1 + \left(\frac{(\omega_{ce}/\omega)\sin^2\theta}{2(1-\omega_{pe}^2/\omega^2)\cos\theta}\right)^2\right]^{1/2}$$

α Polarization factor

H.Soltwisch, PPCF, 1993

Comparison between experiments and analytic calculation

Using Jone Matrix and WKB to calculate phase difference in the lowest order when φ_{CM}^2<<1

$$\varphi_R - \varphi_L = 2\varphi_{FR} - \frac{1}{3}\varphi_{FR}\varphi_{CM}^2$$

Coupling effect is verified on DIII-D

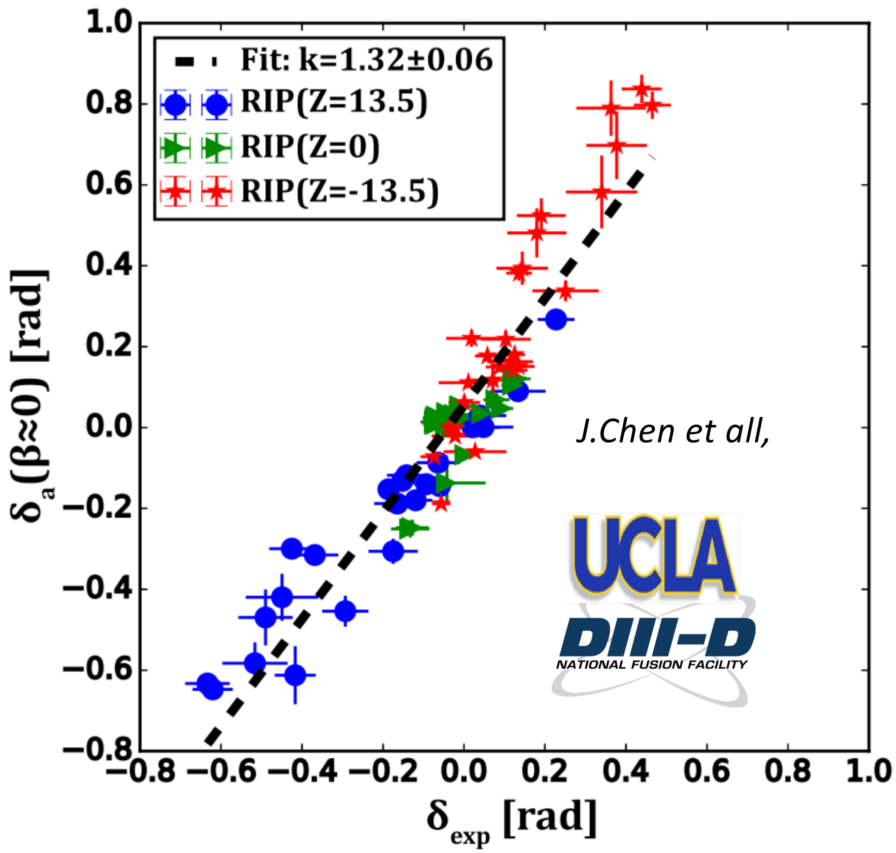

J.Chen,W.X. Ding, D.L. Brower, PPCF (60),085001(2018)

Part III: (c) Coupling between Interferometer and Faraday Rotation for three wave system

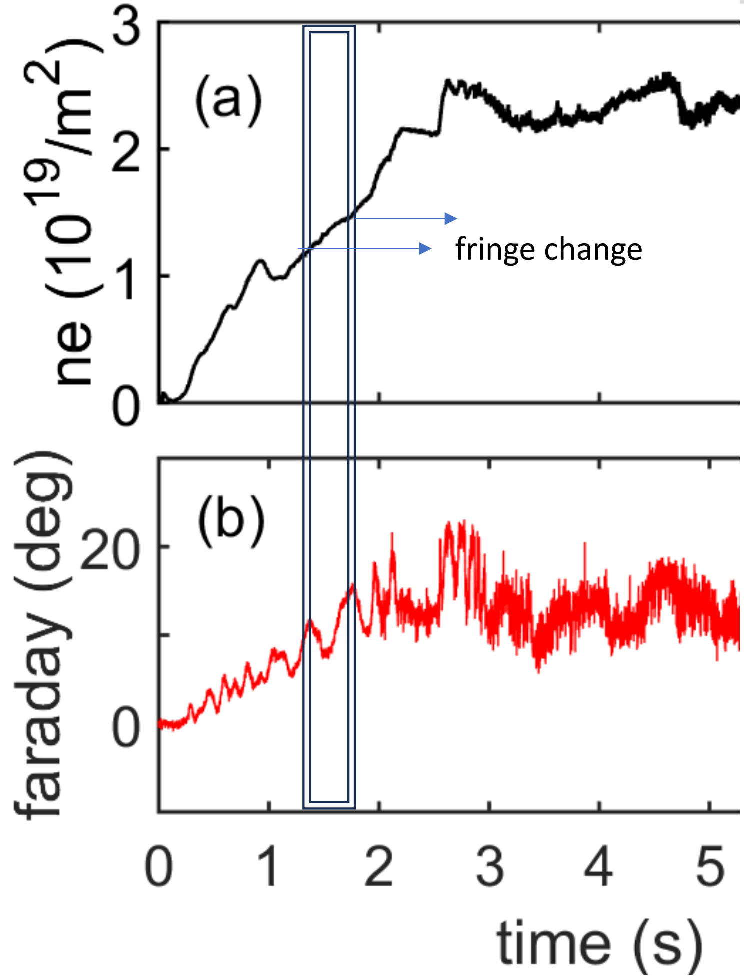

$$\varphi = -\lambda\, r_e \int n_e\, dL$$

$$\boldsymbol{\Psi_F = 2.62\times10^{-13}\lambda^2 \int n_e B_z dl}$$

It is often observed when density ramps up on EAST, Faraday rotation shows oscillations with a period corresponds to a fringe of interferometer.

Density measurement impacts on Faraday measurement

Probe beams with small amount of unwanted signals

$$E_{L1} = A\cos(\omega_L t + \varphi_L) + \varepsilon A\cos(\omega_L t + \varphi_{LS})$$
$$E_{R1} = A\cos(\omega_R t + \varphi_R) + \varepsilon A\cos(\omega_R t + \varphi_{RS})$$

Unwanted signals

$\varepsilon \ll 1$ *Stray lights* $\quad \phi_I = (\varphi_R + \varphi_L)/2$

$\phi_{FR} = (\varphi_R - \varphi_L)/2$ Faraday Rotation

$\phi_{FS} = (\varphi_{RS} - \varphi_{LS})/2$

$$I = (E_{L1} + E_{R1})^2 \sim 2A^2\cos[(\omega_R - \omega_L)t + (\varphi_R - \varphi_L)] + \varepsilon A^2\cos[(\omega_R - \omega_L)t + (\varphi_R - \varphi_{LS})] + \varepsilon A^2\cos[(\omega_L - \omega_O)t + (\varphi_{RS} - \varphi_L)]$$

Measured Phase shift including very little unwanted light：

$$\Psi = \arctan\frac{\sin 2\phi_F + 2\varepsilon\cos(\phi_I - \phi_{IS}) \times \sin(\phi_F - \phi_{FS})}{\cos 2\phi_F + 2\varepsilon\cos(\phi_I - \phi_{IS}) \times \cos(\phi_F - \phi_{FS})}$$

$$\Psi \approx 2\phi_F - 2\varepsilon\cos(\phi_I - \phi_{IS}) \times \sin\phi_{FS}$$

Density dynamics impacts on Faraday rotation measurement due to a small amount of stray light. It is also true for Cotton-Mouton Polarimetry.

Z.Y.Zou, et al Review of Scientific Instruments ,2018,vol.89:013510
H Lian, Y Q Chu, et al. RSI,2019, 90: 053501.

Stray light affects Faraday rotation

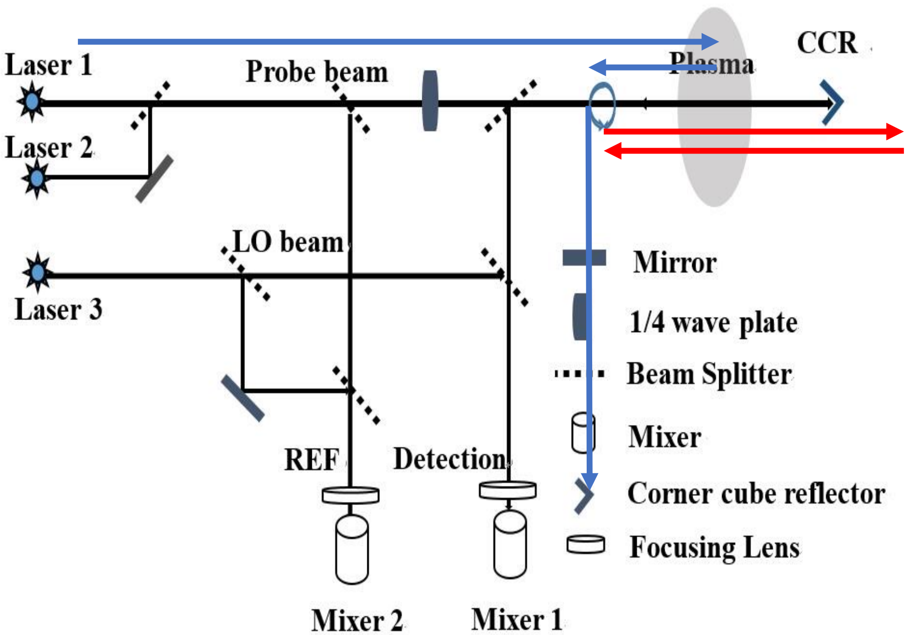

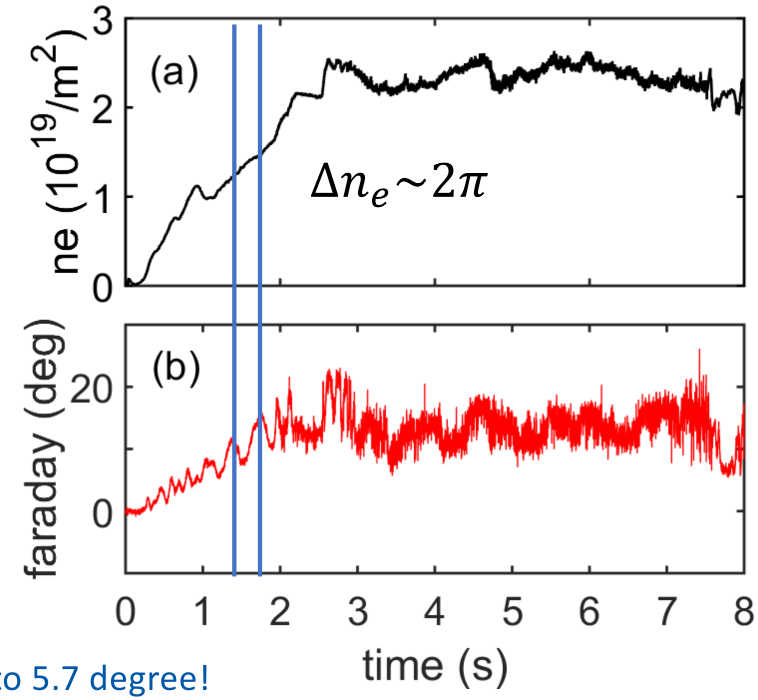

Probing light (red line)

Stray light (blue line)

ε=10%, corresponding to 5.7 degree!

$$\Psi \approx 2\phi_{FR} - 2\varepsilon \cos(\phi_I)$$

Stray light control is important for any polarimetry

Summary

- Interferometer;
- Faraday effect Polarimetry;
- Cotton Mouton effect;
- Technique Notes

(a) Temperature effect on dispersion relation of EM;

(b) Coupling between Faraday and Cotton Mouton effects;

(c) Coupling between Faraday rotation and Interferometer.

Additional references

1. S. K. Sheem, J. Appl. Phys. 52, 3865 (1981).
2. J. Macdonald, S. N. Bland, and J. Threadgold, Rev. Sci. Instrum. 86, 083506 (2015).
3. S. Zhang, C. Chen, T. Lan, et al., Rev. Sci. Instrum. 91, 063501 (2020).
4. T. Lan, S. Zhang, W. Ding, et al, Rev. Sci. Instrum. 92, 093506 (2021).
5. C. Chen, T. Lan, C. Xiao, et al, Plasma Sci. Technol. 24, 045102 (2022).
6. T. Lan, Z. Bai, H. Zhang, et al., Rev. Sci. Instrum. 95, 103514 (2024).
7. H.Q.Liu, et al. *Rev. Sci. Instrum.* 87, 11D903 (2016)
8. Z.Y.Zou, et al. *Fusion Engineering and Design* 112 (2016) 251–256.
9. Z.Y.Zou, et al. *Rev. Sci. Instrum.* 87, 11E121 (2016)
10. Z.Y.Zou, et al. *Rev. Sci. Instrum.* 87, 11E121 (2016)
11. H.Lian, et al. *Rev. Sci. Instrum*. 90, 053501 (2019)
12. W. F. Bergerson, P. Xu, J. H. Irby, D. L. Brower, W. X. Ding and E. S. Marmar, Review of Scientific Instruments 2012 Vol. 83 Issue 10
13. J. Chen, W. X. Ding, D. L. Brower, D. Finkenthal and R. Boivin, Rev. Sci. Instrum. 2018 Vol. 89
14. W. X. Ding, D. L. Brower, W. F. Bergerson and L. Lin, Review of Scientific Instruments 2010 Vol. 81 Issue 10
15. W. X. Ding, D. L. Brower, B. H. Deng and T. Yates, Review of Scientific Instruments 2006 Vol. 77 Issue 10
16. W. X. Ding, H. Q. Liu, J. P. Qian, D. L. Brower, B. J. Xiao, J. Chen, et al. Review of Scientific Instruments 2018 Vol. 89 Issue 10
17. L. Lin, W. X. Ding and D. L. Brower, Review of Scientific Instruments 2012 Vol. 83 Issue 10
18. W.X.Ding, H.Q.Liu, et al. Rew. Sci.Instrum. Vol.89,2018
19. T. Akiyama, K. Kawahata, S. Okajima and K. Nakayama, Plasma and Fusion Research 5 (2010)S1041.
20. T.Akiyama*, et al.* Rev. Sci.Instrum. Vol.87, 11E133(2016).
21. V.P.Drachev, et al. Rev.Sci.Instrum. Vol.64,1010(1993).
22. M.A.Van Zeeland, *et al.* Rev.Sci.Instrum. Vol.84.043501(2013).